THE EFFECTIVENESS OF
WATER RUDDERS ON FLYING BOATS

by

L. B. Libbey

Experimental Towing Tank
Stevens Institute of Technology
Hoboken, New Jersey

THE EFFECTIVENESS
OF WATER RUDDERS
ON FLYING BOATS

A Thesis Submitted in Partial Fulfillment

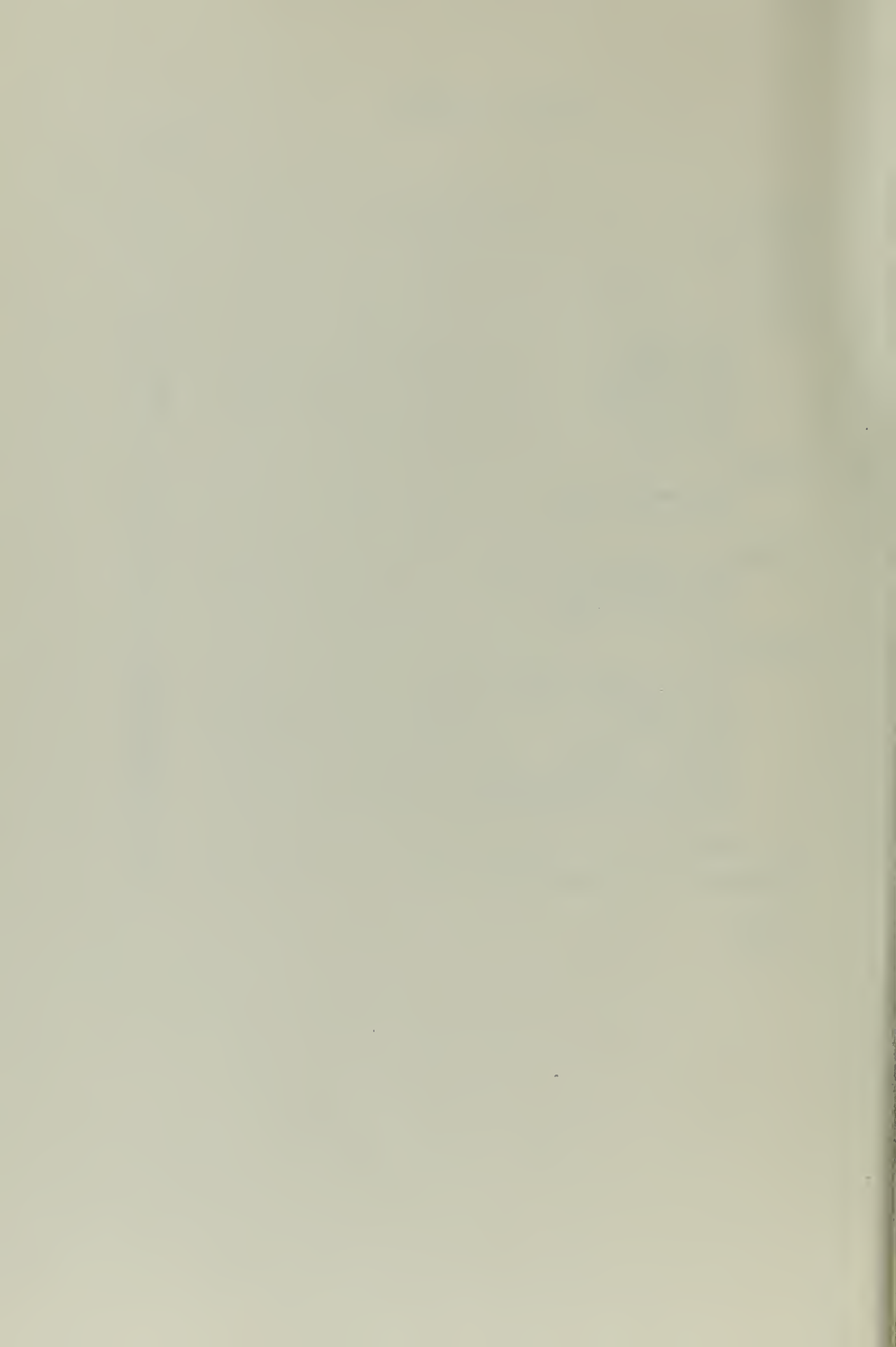of the Requirements for the Degree of

Master of Science

STEVENS INSTITUTE OF TECHNOLOGY

Submitted by Lester Blaine Libbey

TABLE OF CONTENTS

SUMMARY

The effectiveness of water rudders on flying boats is investigated by model-testing three rectangular rudders of aspect ratios 0.5, 1.0, and 2.0 for their lift forces developed when located beneath the vee-bottomed afterbody keel near the sternpost of a conventional military flying boat. Flying boats have always depended upon the asymmetrical thrust of their multiengines for maneuvering at low speeds, but recent development of high length-beam ratio hulls has stirred interest in a simple and more effective control.

Yawing tests are reported both with and without rudders, and from them the forces of the rudders, the effects of an opening gap, and of wake at yaw angles are discussed. It is found that a low aspect ratio (0.5) rudder is superior to higher aspect ratio rudders in maximum lift, burble point delay, sensitivity to disturbances which follows from low lift curve slope, effective aspect ratio, and in obstruction offered on the beach.

The gap caused by a rudder opening below a vee-bottom is found to increase the effective aspect ratios 28 and 20% for geometric aspect ratios of 0.5 and 1.0, respectively. This may be compared to a 100% gain which would be obtained if there was complete reflection from the surface above the rudder.

The wake is found to disturb the flow over the rudders but little for yaw angles up to 7 degrees tested in this work.

1
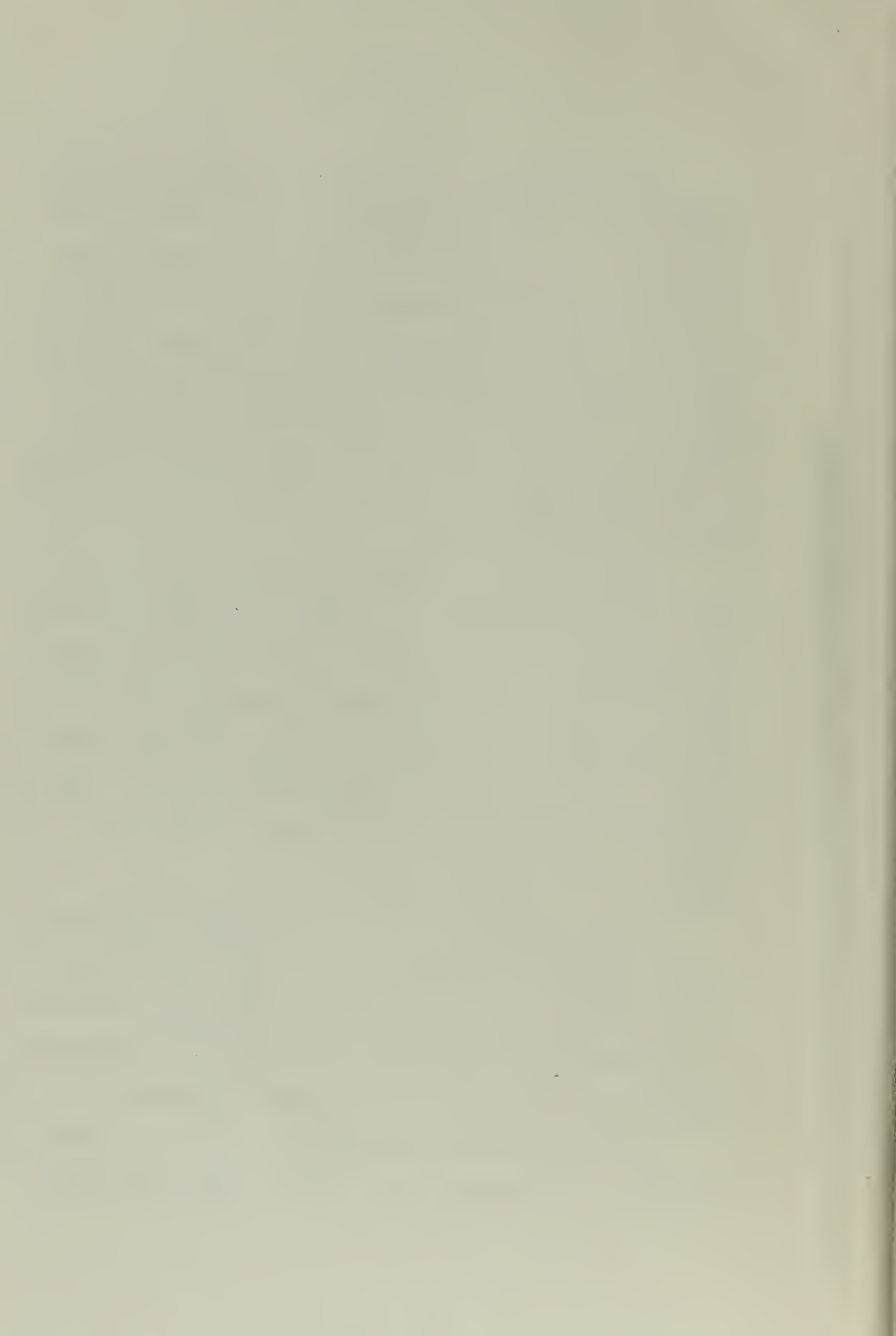
INTRODUCTION

The problem of maneuvering large flying boats at low taxiing speeds has always caused concern, and is receiving renewed attention today with the advent of long afterbody hulls. It is one of directional stability in the displacement, or low speed range, and has been treated by Pierson (29, 30), Locke (26,27), and many others (16, 17, 18, 22, 23, 24, 25, 33, 34).

The difficulty arises with the instability encountered when the boat is moving very slowly. It has been described by Korvin-Kroukovsky (5) as being due to the hull acting as a displacement vessel at the low speed of taxiing with conditions above and below the water line combining to make it unstable. There is deep draft in the forebody sections forward of the center of gravity, and a smaller draft and submerged side area aft. Above the water surface the greater side area lies aft of the center of gravity and includes the tail surfaces. In the case of a small yaw, say due to a side gust, both of these conditions tend to make the craft unstable in yaw, in this case, to "weathercock".

Flying boats, as differentiated from single-engine seaplanes which use water rudders, have depended completely on the asymmetrical power derived from their multi-engines for turning at low speeds. However, Locke (42) reports that in the past few years about 10 per cent of all on-the-water accidents to

flying boats without reversible pitch propellers could be attributed to lack of a water rudder. These include running into breakwaters, ramps, buoys, moored aircraft, and the like. The trouble here seems to be that when the aircraft approaches danger, the pilot applies additional power to turn, but in so doing he speeds up and crashes into the object he was trying to avoid.

Reversible pitch propellers appear to be the ideal answer to controllability at low speeds. Chillson (36) and Hutchinson (25) both show the advantages inherent with the negative thrust available here. However, Locke (42) states that although maneuvering accidents should be a thing of the past, it even takes a certain amount of time to reverse pitch, and maneuvering with the aid of the propellers may be slightly awkward with twin-engine flying boats. At any rate the desirable results looked for with reversible pitch propellers have not yet been realized in common practice, and simpler answers are still in demand.

Many devices have been and are being tested as a solution to this embarrassing situation. Sea anchors have long been used with some success, but the delays in relaying orders aft for their effective use leave much to be desired. New ideas include varieties of flaps on the bottom, outboard motors, and rudders.

As mentioned above, water rudders have been used by single-engine seaplanes for years with success. It is apparent
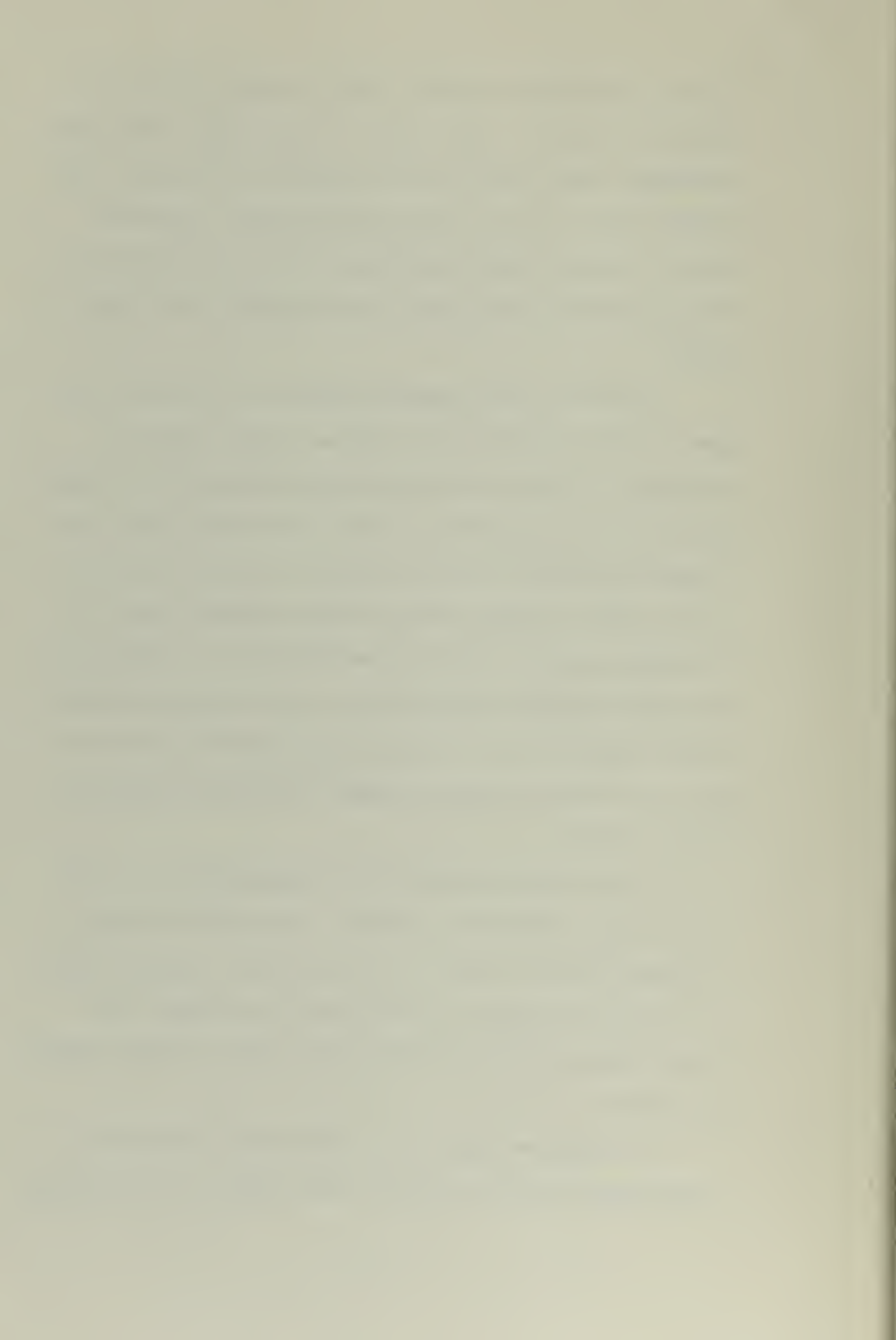
that the air rudder is of no use at low speeds due to lack of sufficient air flow over its surfaces. Locke (42) states that when asymmetrical power is not available, the simplest and most positive means of providing directional control appears to be a water rudder.

Little systematic study has been given to the forces available from water rudders on flying boats. A rough correlation of the dimensions of water rudders of various actual seaplanes and flying boats as related to their behavior was presented by Locke (42). However, a wealth of accumulated data is available from surface ship rudder investigations (35,37,38, 39, 41, 43, 44). Of particular value is Darnell's work (37) which is a complete study of the hydrodynamic characteristics of rudders. His results are used later in this report for comparisons.

The case of a water rudder located beneath the afterbody keel, far aft of the step near the sternpost, is investigated here. It is realized that this location is not good for ground clearance on the beach, and that the rudder should be retractable, but the advantages hydrodynamically to be gained here were controlling. In this location the rudder is completely immersed in comparatively undisturbed water, and the effective aspect ratio should be greater than the actual geometric aspect ratio. Both of the foregoing should benefit the rudder's "lift".

Two differences from the surface ship rudder problem be-

come evident here. The first is the gap effect due to the vee-bottom of a flying boat. Although the rudder may be flush against the keel in the fore and aft position, as it turns, it opens a gap which destroys some of its "reflected" aspect ratio gains. Secondly, because a flying boat may run in a yawed attitude as a "steady condition", the flow past the rudder may be altered from the airplane's centerline appreciably. These effects are studied.

The general purpose of this investigation is then: to estimate what the rudder should do, to measure what it can do, and to offer results that may be of use to designers in selecting a rudder for their particular need. In addition, a bibliography is offered containing many works in fields allied to this subject.

Several limitations were necessarily established in order to arrive at tangible results in the time available. Only rectangular rudders of three representative aspect ratios were tested. The four speeds used were equivalent to full scale values of from 5-1/2 to 17 knots. Only one rudder location was used, as mentioned above. One vehicle or hull type was used, that being a well-known military flying boat hull, which has generally good directional stability. Other variables held constant here include: load, trim moment, heel angle, rudder area, and initial gap.

Further limitations to this study are made as regards

the methods used. Any turning analysis of a free craft is a dynamic problem and of the type that can be handled by a rotating arm apparatus, such as operates at the Experimental Towing Tank, Stevens Institute of Technology, Hoboken, New Jersey. For this limited work only the tendency to turn, or the initial stage of the turn, as represented by a model towed straight down a tank in a yawed attitude was investigated. As Pierson (29) has explained, it is a fact that the yawing moment versus yawing angle curves must undergo radical changes once the turn has been started.

It should be made clear that although yawing moment coefficient versus yawing angle (C_{n_ψ} vs. ψ) curves were made with the rudders tested, this study does not attempt to cover the prehump directional stability problem which is of a different nature than that of low speed maneuvering. It is a very important one because of its bearing on take-offs. Pierson (30) has discussed this problem with excellent detail. Although he considers the effects of skegs (fins) and chines, he does not mention the use of rudders. Locke (7) mentions that if prehump directional instability manifests itself, it can be corrected by cutting back the power on one or more of the outboard engines of a multi-engine flying boat in order to introduce an asymmetric thrust. The idea immediately suggests itself to use a water rudder to obtain this asymmetric motion without cutting back any power. This has not been investigated in this report,

although it should be looked into.

Briefly, the rudders were tested to determine their lift, or cross-wise force, by measuring the yawing moment coefficient resulting from their position at various speeds, and then converting it to lift coefficient. The result being lift versus angle of attack (C_L vs. α) curves for each rudder and speed.

The most significant conclusion reached in these tests is that a low aspect ratio (0.5) rudder is the most effective of the three tested for use with a flying boat hull. This statement is based on the low aspect ratio rudder's having the highest maximum lift, most delayed burble point, least sensitivity to yaw disturbances, which is a direct result of it having the lowest lift curve slope, greatest gain in effective aspect ratio, and least projection below the keel structurally.

Other conclusions include gap effects and variation of effective aspect ratio gains with geometric aspect ratio. The gap that opens beneath the vee-bottom is shown to reduce considerably the effective aspect ratio gain found with a no-gap condition. The effective aspect ratio gains decrease progressively from plus 28% for A = 0.5 to minus 2.6% for A = 2.0.

The rudder location used proves effective with small wake effects, large moment arm, and complete immersion for the low speed range.

The problem of how effective water rudders are for flying boats is still unanswered completely at the end of this

particular investigation, for two reasons mainly. The first is a lack of comparison with other devices for maneuvering at low speeds, and the second is the lack of dynamic testing at various turning radii. Further testing should also be done on the newer planing-tail type hulls.

All testing was performed in Tank No. 1 of the Experimental Towing Tank, Stevens Institute of Technology, Hoboken, New Jersey during the months of February, March, and April, 1950.

Acknowledgment is appreciatively made to all of the staff of the Experimental Towing Tank who helped with the work in many ways. Especial mention is given to Professor B. V. Korvin-Kroukovsky for his very valuable and patient advice at every turn.

Non-dimensional Coefficients:

Load Coefficient $\qquad$ $C_\Delta = \Delta/wb^3$

Speed Coefficient $\qquad$ $C_V = V/\sqrt{gb}$

Trimming Moment Coefficient $\qquad$ $C_M = M/wb^4$

Yawing Moment Coefficient $\qquad$ $C_{M\psi} = M_\psi/wb^4$

Heave Coefficient $\qquad$ $C_h = h/b$

Lift Coefficient $\qquad$ $C_L = L/\frac{1}{2}\rho V^2 S$

Normal Force Coefficient $\qquad$ $C_N = N/\frac{1}{2}\rho V^2 S$

Other Symbols:

A $\quad$ Aspect ratio $= \ell^2/S$

C $\quad$ Coefficient

H $\quad$ Hull alone

L $\quad$ Lift of rudder, pounds

M $\quad$ Moment, foot-pounds

N $\quad$ Normal force of an airfoil

N_R $\quad$ Reynolds number $= \dfrac{\rho V c}{\mu}$

R $\quad$ Rudder alone

S $\quad$ Area of rudder, inches^2

T $\quad$ Total

V $\quad$ Velocity, feet per second

a $\quad$ Rudder arm, distance from center of gravity to rudder stock parallel to baseline

b $\quad$ Beam of main step, feet

c   Chord of rudder, inches

g   Acceleration of gravity, 32.2 feet per second^2

h   Heave at center of gravity (height above position at rest and zero trim angle), feet

i   Initial value

ℓ Span of rudder, inches

m   Model

o   Standing value

q   Dynamic pressure $= \frac{1}{2} \rho V^2$, pounds per inch^2

r   Running value

s   Full scale

w   Specific weight of water, 62.3 pounds per foot^3

α_H Angle of attack of rudder from hull center line, degrees

α Angle of attack of rudder

Δ Load on water, pounds, or change in

ϵ Additional angle due to angular velocity, degrees

λ Ratio of model to full scale dimensions

μ Coefficient of viscosity of fresh water, here: 0.851 x 10^{-5} slugs per foot-second at 70 degrees, Fahrenheit

υ Kinematic viscosity of fresh water, here: 0.449 x 10^{-5} feet^2 per second

ρ Density of fresh water, 1.94 pound seconds^2

τ Trim angle, degrees

ϕ Heel angle, degrees

ψ Yaw angle, degrees

The Rudders.

The three water rudders tested were all rectangular in plan form, constant at one square inch area, and different in aspect ratio. The aspect ratios chosen were: 0.5, 1.0, and 2.0, which determined at once the profile dimensions. The thickness ratios were 0.140, 0.125, and 0.100 respectively. All sharp corners were rounded, and the profiles were streamlined symmetrically. The maximum thickness and the axis of the rudder stock were set at the quarter-chord position. These rudders are shown in Fig. 1.

The rudders were designed rectangular in form as that is a fairly general case, and also because Winter (57) has shown forces to be similar on both rectangular and elliptical plan forms of equal aspect ratio and angle of attack. Darnell (37) showed identical lift slopes in the linear range for various plan forms at the same aspect ratio; the differences in the curves all occurred in their shapes at maximum values.

They were taken equal in area, and one square inch in area, for better comparison and to obtain a unit lift value which could be adjusted to suit a particular need. The aspect ratios cover the range of short span air- or hydro-foils which is common in rudders.

The thickness ratios were chosen arbitrarily to keep the

11

greatest thickness which occurs at an aspect ratio of 0.5 within reasonable bounds. It should not be too thick if the rudder is to be retractable. Fischer (38) stated that a thickness ratio of 0.2 would give the greatest lift, but Darnell (37) found that the differences in lift coefficient for rudders of various thickness ratios with the same aspect ratio were negligible.

The rudders were cut and filed to shape from brass stock, and were smoothed with emory cloth.

The Vehicle.

The rudders were tested on a 1/22 scale model of a well-known military flying boat. This aircraft has "conventional" lines, that is to say, it is not of the newer planing-tail type. It is also known to be generally good for low-speed maneuvering, so that the testing of the rudders was not radically affected by the vehicle. An extension of the tests to one of the newer hulls would provide further excellent data for comparisons.

The rudders were located at the keel, 15 inches aft of the center of gravity, or 13 inches aft of the step. These distances correspond to 27.5 feet and 23.8 feet, respectively, for the full-scale case as shown roughly in Fig. 2. This location places the rudder near the end of the afterbody for maximum moment arm, and below the keel for relatively undisturbed, or "green water" flow. The rudders were completely immersed for all speeds tested.

The model rudder stocks extended through and above the hull, perpendicular to the afterbody keel, which made them vertical for 7.5 degrees trim, a good displacement range trim. Above the deck, the rudder stocks fitted into a pointer which indicated on a protractor the rudder angle setting relative to the centerline. Fig. 2a shows the arrangement roughly.

The Apparatus.

The model, or vehicle, with a rudder was mounted on the standard seaplane yawing apparatus of the Experimental Towing Tank, described by Locke in (26), and shown schematically in Fig. 3. The model was mounted on pin bearings at its center of gravity, and was thus allowed freedom in trim, or pitch. The yoke could be adjusted to give fixed heel angles. The yoke was attached to a staff which allowed freedom in yaw. The angular motion of the staff was restrained by a calibrated spring, thus allowing determination of the yawing moment. A dashpot was provided for damping the yaw. Freedom of heave, or vertical freedom was also provided by balanced, pivoting beams from the carriage to the model, and by applying the towing force from a point well forward of and parallel to the center of gravity.

The calibrated spring mentioned above constituted the yawing dynamometer. The spring was relatively weak in order to respond to small yaw moments, and give a deflection that could be easily read. It should be noted that this method of using a

13

spring makes it difficult to obtain the moment curve near a dis-
continuity, and impossible to get points on any portion of a
curve with a higher slope than the spring constant. However,
no discontinuities were approached in the range tested here for
rudder use. An example of this type of curve may be seen in
Fig. 14 for a high speed test made only to compare with pre-
vious tests.

The Tow Tank.

All tests were made in Tank #1 of the Experimental Tow-
ing Tank, Stevens Institute of Technology, Hoboken, New Jersey.
This model basin is 109 feet in length and 9 feet in width. It
is semi-circular in cross-section. This facility has advantages
of simplicity of operation, and exactness of pre-set speeds.

The Method.

The method used was essentially that in common practice
at the Experimental Towing Tank, and as described by Locke
(26). The yawing test method was extended in this case to give
values of rudder lift, and the computations involved are ex-
plained in a section that follows.

PROCEDURE OF TESTS

The Yawing Tests.

Routine yawing tests were made both with and without a rudder. One test was made without a rudder at a higher speed than shown in Table I, namely: $C_V = 2.17$, or $V_S = 27$ kts., in order to compare this investigation with the original tests on the same model. (Reference is classified.)

Bare hull yawing tests were made for the four speeds used throughout. The rudder of $\Lambda = 1.0$ was then mounted and tested at settings of rudder angles: 0, 10, and 20 degrees.

In these tests no heel angle was introduced to simulate a wing tip down. A small nose-down moment was maintained to partially simulate thrust effects ($C_M = -0.038$). The model was ballasted for a value of $C_\Delta = 0.8$, and was allowed to pivot freely about both the transverse and vertical axes. These are average conditions used by Pierson (29).

The Rudder Tests.

The three rudders (Fig. 1) were tested at four representative speeds. Table I shows the values in dimensional and non-dimensional forms. The speed coefficients range from 0.521 to 1.600, and correspond to full scale values for the aircraft used of from 5.55 to 17.03 knots.

Each rudder was mounted on the model, and the yawing

angle recorded (the initial yaw angle being zero) for various rudder settings at each of the four speeds. A running plot of yawing moment versus rudder angle was kept to insure that sufficient runs were made to include the burble, or stalling, point for each speed. The angle of trim and heave were also noted for each run.

The reduction of these data are described in the following section.

The Calibration Curves.

Figs. 17, 19, and 20 are calibration curves used in the reduction of the test results, and will be mentioned by way of introduction.

Fig. 17 is the usual spring curve drawn preparatory to making yaw tests. Fig. 19 is also a spring curve expressed in different units. For each a known weight on a string was hung over a pulley and hooked to the bar at the center of the spring, shown in Fig. 3. In this case the weight was hooked to the bar at a distance from the center of gravity (staff center) equal to the distance from the center of gravity to the rudder stock (quarter-chord of rudder, or approximate center of pressure), so that the weight or force was plotted against the resulting yaw angle in Fig. 19 directly as lift at rudder versus change of yaw angle, L vs. $\Delta \psi$.

This force multiplied by its arm, or distance from the center of gravity becomes the yaw moment, and when divided by wb^4 becomes the non-dimensional yawing moment coefficient. The latter was then plotted against change of yaw to give Fig. 17 with C_{M_ψ} vs. $\Delta \psi$.

Fig. 20 is a replotting of Fig. 17, but with the addition of the lift coefficient, C_L, also versus the change of yaw angle, $\Delta \psi$. The C_L values were obtained for each of the

four speeds used, with the lift values of Fig. 19, the density
of fresh water, and the area of the rudders.

The Yawing Tests.

The yawing tests outlined in the Procedure of Tests sec-
tion were made according to established Experimental Towing
Tank methods. The yawing moment coefficient versus yaw angle,
C_{M_ψ} vs. ψ, values were computed using the calibration curve,
Fig. 17, and the running yaw angle obtained from the formula:

$$\psi \equiv \psi_r = \psi_i + \Delta \psi \qquad (1)$$

where, ψ_r running angle of yaw;

ψ_i initial angle of yaw;

$\Delta \psi$ change in angle of yaw.

The results are plotted as Figs. 14, 15, and 16.

Fig. 14 is an especially graphic means of showing the
variance of directional stability characteristics as a function
of speed, angle of trim, and pitching moment. It was developed,
and is described by Locke (26). It is sometimes referred to as
a "wallpaper" chart for obvious reasons.

Fig. 15 is the conventional yawing moment versus yaw
angle curve for $C_V = 1.041$, but with the curve for the hull plus
the rudder of $A = 1.0$ at zero angle of attack with respect to
the hull superimposed.

Routine yawing tests were also made at $C_V = 1.041$ with
the rudder of $A = 1.0$ set at 10 and 20 degrees with respect to

the hull center-line. The curves for these tests are shown in Fig. 16.

The Rudder Tests.

The aim of the rudder tests was to obtain lift curves for the rudders in terms of C_L vs. $\propto$. These were obtained using the yawing apparatus in a similar manner as in the yawing tests, and by using the results of the yawing tests also.

The steps used for obtaining one curve for one rudder and one speed will be described. With the rudder mounted on the model, and the rudder angle with respect to the hull, $\propto_H$, noted, a yawing run was made at the desired speed, with the model's initial yaw angle, ψ_i, always zero. This gave a value of $\psi \equiv \psi_r$ which for these tests always equalled $\Delta \psi$, since $\psi_i = 0$.

This value of ψ , being for the hull plus the rudder, was labelled ψ_T. From Fig. 17, a corresponding value of $(C_{M_\psi})_T$ was obtained.

A value of C_{M_ψ} for the bare hull, without a rudder, was obtained from the yawing tests, Fig. 14, for the same   , and this was called $(C_{M_\psi})_H$.

Subtracting the value for the hull alone from the total value gave the rudder alone value, Fig. 18, as:

$$(C_{M_\psi})_T - (C_{M_\psi})_H = (C_{M_\psi})_R \qquad (2)$$

Fig. 20 was then used to convert $(C_{M_\psi})_R$ to C_L of the

rudder. An example in the use of Fig. 20 is shown, entering at "a" and proceeding via "b", "c", to "d".

Other points were obtained similarly at other rudder angles, α_H. It then remained only to correct α_H to a true angle of attack, α, with respect to the fluid flow. For this correction, it was assumed that the flow past the rudder was unaffected by the yaw angle of the hull, or:

$$\alpha = \alpha_H - \psi \qquad (3)$$

The resulting lift curves for the three rudders, and each at the four speeds, were found in this manner and plotted in Figs. 4, 5, and 6. Working values for each point were recorded in Tables III, IV, V, and VI. A plotting point code is shown in Table I.

Lift and Aspect Ratio.

The C_L vs. α curves obtained (Figs. 4, 5, and 6) are shown to be practically straight lines until the region of burbling (or stalling) is approached. In the burbling region they round off, or flatten out, before breaking for aspect ratios of 1.0 and 2.0. For A = 0.5, the rounding is less and the breaking is sharper than in the other two cases. In every case the curves are found to collapse very well, which is to say, they have practically the same slope for the four speeds tested at the same aspect ratio.

In general, the effects of aspect ratio are found to be the most pronounced for comparing other parameters. Von Mises (55) has written that the lift coefficient is almost entirely proportional to angle of incidence and aspect ratio. Winter (58) goes further to say that the flow pattern is practically independent of Reynolds number.

Perhaps the most evident effect of aspect ratio is the slope of the C_L vs. α curve. It is seen in Fig. 7 for a constant speed that slopes vary from 0.0242 for A = 0.5, to 0.0530 for A = 2.0. This is also shown similarly by Darnell (37) in his Fig. 26. This effect is well-known for airfoils of greater aspect ratios, and it is of interest to compare the results obtained here with airfoil theory and wind tunnel experimentation.

There are many expressions in the literature for this lift curve slope, or $dC_L/d\alpha$. References (45) through (60) all pertain to this subject. Siler (56) correlated most of the existing theory of low aspect ratio lifting surfaces, and developed a simple expression for determining the lift of low aspect ratio, thin, flat, rectangular airfoils, completely immersed in a fluid:

$$C_N = \frac{2 \pi A \sin\alpha \cos\alpha}{2 + A} + 2 \sin^2\alpha \tag{4}$$

where the first term accounts for the longitudinal flow found for all aspect ratios, and the second accounts for the cross-flow taken from Bollay (45) at zero aspect ratio. Winter (58) in his "Danzig experiments" made unusually complete tests over the low aspect ratio range. Bollay (45) accounted for the non-linearity of Winter's results, and developed very complicated formulas which agreed well with them, but are not easy to use.

Assuming an angle of attack of 10 degrees for an aspect ratio of unity, values of lift coefficient from the above theory were computed, and are listed below with the experimental results of Darnell (37) and these tests.

From Siler (56)	$C_N = 0.42$	$C_L = 0.413$
Winter (58)	$= 0.41$	$= 0.404$
Bollay (45)	$= 0.50$	$= 0.492$
Gottingen experiments (45)	$= 0.39$	$= 0.384$
Lifting line theory (45)	$= 0.38$	$= 0.374$
Von Mises (55)		$= 0.333$

From Darnell (37), for experimental tests of rudders under a
flat-bottomed model, when the rudder was flush against the
bottom: $C_L = 0.447$
when one-third of its span away from the bottom:

$$C_L = 0.335$$

From these tests, Table II and Fig. 5, under a vee-bottomed
flying boat hull, which caused varying gap:

$$C_L = 0.375$$

An inspection of the values above shows that the result
of this testing is between Darnell's "no gap" and "with gap"
figures, and is in the range of the various theoretical values,
which are assumed to be "no gap" predictions.

The von Mises (55) value, used above, was obtained from
a simple formula found to represent airfoil experimental re-
sults fairly well. It is, at any rate, sufficiently accurate
for use here without going to the more exact and long expres-
sions of Bollay and Siler. This formula has also been used
with success by Korvin-Kroukovsky and follows:

$$\frac{dC_L}{d\alpha} = \frac{0.1}{1 + 2/A} \tag{5}$$

For further graphical analysis, all slopes of the lift
curves from Figs. 4, 5, and 6 are plotted against actual aspect
ratio in Fig. 9. Other points are added from the experimenta-
tion of Darnell (37) and an M.I.T. thesis (42A) mentioned there-
in.

The aspect ratios used in these tests, 0.5, 1.0, and 2.0 cover a border-line range for which neither very low aspect ratio theory nor ordinary airfoil theory applies exactly. For comparative purposes, Equation (5) is plotted in Fig. 9 also. An "effective" aspect ratio, A_e, is then obtained by projecting the actual points to the A_e curve at the same $dC_L/d\alpha$. They are plotted in Fig. 10, and recorded in Table II. It is seen that the effective aspect ratios are slightly greater than the actual aspect ratios of 0.5 and 1.0, and are slightly less than the actual aspect ratio of 2.0. This tendency is similar to the results of Darnell (37), and far from a value of twice the geometric or actual aspect ratio that might be expected from "reflection" theory for no gap.

As a criterion for selecting an effective rudder, the slope of its $dC_L/d\alpha$ curve is important, and a low value appears to be the most desirable. Fischer (38) explains it this way:

> "The best distribution of rudder area is obtained when aspect ratio is approximately 1.3 -
> 1.0 because with such rudders, the rudder forces
> for small rudder angles used in normal steering
> do not increase too rapidly, yet large forces
> are developed at a rudder angle of 30 degrees."

Looking at the flying boat problem in particular, another reason for the desirability of low slope is evident. Flying boats have a tendency to yaw rather suddenly to rather large angles, so that the actual angle of attack of a rudder far from the center of gravity could build up or decrease rapidly. In

this case, the rudder with a high lift slope would stall where one with a low slope might still be effective.

The point of the preceding paragraph can be grasped vividly with the aid of Fig. 17. This is an exaggerated vector diagram which shows the effect of the introduction of a yaw angle, ψ, with its angular velocity, r, on the actual angle of attack of the rudder. It is seen that the instantaneous velocity at the rudder, V_R, is the vector sum of the hull's forward velocity, V, and the tangential velocity at the rudder, r x a. Also, the instantaneous angle of attack of the rudder, α, is:

$$\alpha = \alpha_H + \psi + \epsilon \tag{6}$$

It must be concluded that the only rudder which will be effective in such a case of rapidly increased angle of attack is one with burble point delayed to high angles, which means a low lift curve slope ($dC_L/d\alpha$).

It is seen from Fig. 7 that the only rudder of these tests which gives large values of lift in the 30 degree range, and at the same time has a low slope to develop the lift slowly is the aspect ratio of 0.5, the lowest tested.

Other effects of aspect ratio are shown in Figs. 11 and 12. The burble point is seen to be delayed by over 10 degrees for A = 0.5 over the other two larger aspect ratios in Fig. 11, and the limits of rudder throw are established thereby. The maximum lift is also considerably greater for the lowest aspect ratio as seen in Fig. 12. These results are considered to

be significant, and should influence the designer of flying boat rudders.

One more interesting result of the lift curves that again points up the desirability of the low aspect ratio rudder is the "scatter" of the points. The comparative lack of scatter for the 0.5 rudder indicates less sensitivity to disturbances which affect slope, the maximum lift, and the burble point. This lack of spread is seen in Figs. 4, 9, 10, 11, and 12, and may be contrasted to the variety of shapes of the lift curves in the burble region for the aspect ratios of 1.0 and 2.0, Figs. 5 and 6. If one considers the effect of a small disturbance in yaw, it is evident that the rudder with the least scatter will react most effectively.

The influence of speed in these tests is less noticeable. Fig. 13 fails to show any increase or decrease of maximum lift with a change in speed. It should be noted that the low speed values were very difficult to obtain due to the very small yaw angles developed. Therefore the resulting low speed points are the least reliable, and show the most divergence from the other speed results.

Gap Effects.

Turning now to gap effects, it is remembered that the location of the rudders is beneath the keel of a vee-shaped afterbody. This means that when the rudder is in a fore-and-

aft position, or zero degrees rudder angle, there is no gap between the top of the rudder and the keel; but as soon as the rudder is turned, a gap opens, increasing in size with increasing rudder angle. It is desired to know the effect of this varying gap on the lift of the rudder.

For a rough analysis, two lift curves were re-plotted from Darnell (37) with one from these tests in Fig. 8. The Darnell rudder was of A = 1.0, and t/c = 0.128; and the tests were made under a flat-bottomed model ship's hull at v_m = 2.5 kts. This compares closely with the rudder of this test: A = 1.0, t/c = 0.125, and v_m = 2.36 kts. although the actual rudder areas of Darnell's tests were 36 square inches. The Darnell rudder was tested for two conditions of hull clearance: 0 and 1/3 span lengths. With the flat bottom this clearance was constant. The three curves in Fig. 8 show the differences in slope, which are numerically: .0447, .0362, and .0335 for the 0-clearance, varying-clearance, and 1/3-clearance, respectively. These values correspond to effective aspect ratios of 1.60, 1.14, and 1.0, respectively. This indicates that the effect of the vee-bottom gap-opening is to reduce the effective aspect ratio reflected gain by about 77 per cent. The angle of deadrise at the rudder location in this case was about 28 degrees. (The deadrise at the keel and step was 20 degrees.) Although this figure is very approximate due to the method of comparison, it is indicative of the great loss in lift due to

vee-bottom of a flying boat. As one means of regaining some of
this loss, the possibility of adding fin area before the rudder
might be explored.

Scale Effect.

The Reynolds number (Vc/ν) for the testing of the
$A = 1.0$ rudder at $C_V = 1.041$ was about 31,500, using the chord
of the rudder (1 inch) as the determining length. However,
since the rudder is operating partially in the wake of the hull,
that is, in water which already has a turbulence corresponding
to the Reynolds number of the hull, it makes it difficult to
decide upon a Reynolds number to represent the turbulence of
the flow about the rudder. It undoubtedly should be much
greater than 31,500.

This raises the question as to just how well the data
obtained here represent full scale conditions. Darnell (37)
discusses this matter at some length in the light of full-scale
wind tunnel tests and other data. He states that up to the
burble point it is fairly safe to say the effect of scale on
the hydrodynamic characteristics is negligible aside from a
small decrease in the profile drag at small angles of attack.
In general, an increase in velocity will shift the position of
the burble to higher angles of attack.

As mentioned above, Winter (58) concludes that for flat
plates (approximately the case here), the flow pattern is prac-

tically independent of the Reynolds number except for small
values (which is not the case in this work).

The Yaw Effects.

As mentioned in the Introduction, this study did not at-
tempt to cover the pre-hump directional stability problem. In
the process of arriving at the rudders' lift curves, C_{M_ψ} vs. ψ
curves were made without rudders. As a matter of interest,
similar tests and curves were made with a rudder affixed. Figs.
15 and 16 show the effect of a rudder at various angles of at-
tack on the yawing moment curves. Fig. 15 shows that merely
adding a rudder at zero angle (a fin or skeg in effect) results
in giving the hull more static directional stability. Fig. 16
shows the additional effects of turning the rudder: the curve
is shifted parallel to itself thus shifting the yaw angle for
zero yaw moment (to the port in the case of starboard rudder),
until the burble point is passed.

Sample Problem.

A very elementary sample problem is introduced to illus-
trate the use of some of the data from these tests. Let it be
proposed to find the size of a water rudder for a flying boat
to develop a yawing moment of 32,000 ft.lb. at 8.5 kts.

Assuming the rudder to be placed 20 ft. behind the cen-
ter of gravity beneath the afterbody keel, the force required

is:

$$L = \frac{32,000}{20} = 1600 \text{ ft.lb.}$$

Using a 0.5 aspect ratio rudder at less than maximum
lift, from Fig. 4, at 30 degrees angle of attack, the lift co-
efficient is:

$$C_L = 0.720$$

From the lift formula,

$$\text{Area} = S = \frac{L}{C_L \frac{1}{2}\rho V^2}$$

$$= \frac{1600}{.72 \times 1.94 \times \frac{1}{2} \times (14.4)^2}$$

$$= 11.1 \text{ ft.}^2$$

and for a rectangular shape,

$$\text{Span} = 1 = (AS)^{1/2} = (0.5 \times 11.1)^{1/2}$$

$$= 2.36 \text{ ft.}$$

$$\text{Chord} = c = S/1 = 11.1/2.36$$

$$= 4.70 \text{ ft.}$$

Lift Curve Construction.

Another use that may be made of these results is the con-
struction of lift curves to meet new and untested conditions.
Starting with the actual aspect ratio of a new rudder, which
need not be even closely rectangular, the slope of its lift
curve may be approximated from Fig. 9, its maximum lift coeffi-

cient may then be obtained from Fig. 12, and its burble point from Fig. 11. With these boundaries, a curve may be arbitrarily faired in the burble region. The action after burble will not be very well determined, but is not too important either. Further, the effective aspect ratio may be obtained from Fig. 10.

Unconsidered Factors.

The variables considered in these tests were limited to speed, aspect ratio, and angle of attack, and initial yaw angle. The results obtained included slope of lift curve, effective aspect ratio, maximum lift coefficient, burble angle of attack, and limited yaw effects.

Many other variables could have been considered, and perhaps should be in future work. The location of the rudder could be varied along the afterbody keel, aft of the sternpost, and even on the bow.

Its initial gap or distance below the hull could also be studied. In this respect, Darnell (37) concluded that all reflected effects were lost at 1/3 of the span's distance below a flat-bottomed hull.

The design of the rudders themselves is open to further testing. Other shapes than rectangular may offer advantages, such as elliptical, or semi-elliptical outlines; or raked leading and trailing edges. The thickness ratio influence may be

explored whether or not a value of 0.20 is best as Fischer (38) reported. On the basis of the work of Winter (58) and Darnell (37) it is thought that these changes will show little effect.

The general hull conditions will certainly affect the rudder action, as for example, the introduction of a planing-tail, or the dipping of a wing-tip float and the resulting heel and drag, or even a change in the deadrise in the vicinity of the rudder. Load and trim are other variables of the hull not considered in this work. But these variables also are not believed to be of great influence.

The influence of the wake turbulence has not been studied here, but the good agreement of the lift curves obtained with previous work (37) leads to the belief that the wake does not seriously affect the rudders in this location.

To adequately determine the effectiveness of water rudders on flying boats dynamic turning tests must be made, as mentioned in the Introduction. This was a much bigger problem than could be entered for this investigation.

Practical problems of design, installation, and control are left for development engineering. They may be considerable if they include retractability, structural strength, and automatic features. It is noted in this regard that the 0.5 aspect ratio rudder favored above for other reasons, is here favorable for its smaller projection beneath the hull which would be an obstruction on the beach.

CONCLUSIONS

The outstanding conclusion of these tests is the superior performance of the lowest aspect ratio (0.5) rudder over the other, higher aspect ratio types for flying boat use. Its effectiveness is better in at least six respects:

1. Highest maximum lift.

2. Most delayed burble point.

3. Least sensitivity to yaw disturbances, which goes with lowest lift curve slope.

4. Greatest effective aspect ratio gain.

5. Least obstruction offered on the beach.

The gap that opens as a rudder with zero initial hull clearance is put over beneath a vee-bottomed hull of about 30 degrees deadrise is found to decrease considerably the effective aspect ratio gain expected by "reflection" effects.

The effective aspect ratio gains appear to drop off as the actual aspect ratio increases. The gains for the 0.5, 1.0, and 2.0 aspect ratio rudders are found to be approximately: plus 28%, plus 20%, and minus 2.6%, respectively.

The rudder location used in these tests, beneath the afterbody keel near the sternpost, is considered to be very good, for the rudder arm is large, the wake effects are small, and the rudders are completely immersed at low speeds (less than 17 knots, full scale).

From the inadequate yawing tests, it is shown how the

33

yawing moment versus yaw angle curve is shifted parallel to it-
self for rudder angles less than the burble point.

REFERENCES AND BIBLIOGRAPHY

Hydrodynamics.

1. Benson, J.M. and Bidwell, J.M. Bibliography and Review of Information Relating to the Hydrodynamics of Seaplanes. NACA Wartime Report No. L-230, 1945.

2. Davidson, K.S.M. Resistance and Powering. Principles of Naval Architecture. v.II. S.N.A.M.E., New York, 1941.

3. Dodge, R.A. and Thompson, M.J. Fluid Mechanics. New York, McGraw-Hill Book Company, 1937.

4. Hunsaker, J.C. Newton and Fluid Mechanics. Journal of Aeronautical Sciences, 1946, v. 13.

5. Korvin-Kroukovsky, B.V. Hydrodynamic Design of Seaplanes. (Unedited Class Notes, S.I.T. Courses F.D. 215-6.) E.T.T., S.I.T., Hoboken, N.J., 1950.

6. Lamb, H. Hydrodynamics. 6th Edition. New York, Dover Publications, Inc., 1932.

7. Locke, F.W.S. Determining the Hydrodynamic Characteristics of Flying Boats. (Aircraft Engineering, 1949, v. 21, n. 242.)

8. Milne-Thomson, L.M. Theoretical Hydrodynamics. 2nd Edition. London, MacMillan and Company, 1949. (Obtainable in New York through Stechert-Hafner, Inc., 31 East 10th Street, New York City 3.)

9. Parkinson, J.B. Appreciation and Determination of the Hydrodynamic Qualities of Seaplanes. NACA T.N. No. 1290, 1947.

10. Prandtl, L. Applications of Modern Hydrodynamics to Aerodynamics. NACA Report No. 116, 1921.

11. Prandtl, L. and Tietjens, O.G. Applied Hydro- and Aeromechanics. New York, McGraw-Hill Book Company, 1934.

12. Prandtl, L. and Tietjens, O.G. Fundamentals of Hydro- and Aeromechanics. Translated by Rosenhead, L. McGraw-Hill Book Company, 1934.

13. Streeter, V.L. Fluid Dynamics. New York, McGraw-Hill
       Book Company, 1948.

14. White   Naval Architecture.

Directional Stability.

15. Arnstein and Klempener. Performance of Airships. Aero-
       dynamic Theory. Edited by Durand, W.F., v. VI, 1934.

16. Axt, W.C. E.T.T., S.I.T. Classified Report No. 323, 1947.
       Prepared for the Glenn L. Martin Company.

17. Axt, W.C. E.T.T., S.I.T. Classified Report No. 326, 1947.

18. Axt, W.C. and Wittke, J. E.T.T., S.I.T. Classified Report
       No. 358, April 1950.

19. Davidson, K.S.M. On the Turning and Steering of Ships.
       Transactions of the Society of Naval Architects and
       Marine Engineers, v. 52, 1944.

20. Davidson, K.S.M. and Schiff, L.I. Turning and Course-
       Keeping Qualities. Transactions of the Society of
       Naval Architects and Marine Engineers, 1946.

21. Gimprich, M. Notes on Forward Motion Stability of Ships.
       E.T.T., S.I.T. TM No. 74, December 1945.

22. Gott, J.P. Note of the Directional Stability of Seaplanes
       on the Water. R. & M. No. 1776, British A.R.C., 1937.

23. Hugli, W.C., Jr. E.T.T., S.I.T. Classified Report No. 182.
       Prepared for the Glenn L. Martin Company, 1942.

24. Hugli, W.C., Jr. E.T.T., S.I.T., Classified Report No.
       275, 1944. For Columbia Aircraft Corporation.

25. Hutchinson, J.L. Note on the Value of Reversible Pitch
       Propellers on Seaplanes. Rep. No. H/Res/178, British
       Marine Aircraft Experimental Establishment, 1944.

26. Locke, F.W.S., Jr. Some Yawing Tests of a 1/30-Scale Model
       of the Hull of the XPB2M-1 Flying Boat. NACA Report No.
       W-66, 1943.

27. Locke, F.W.S., Jr. Bureau of Aeronautics Classified Report No. 1062, May 1948.

28. Perring and Glauert. Stability on the Water of a Seaplane in the Planing Condition. A.R.C. R. & M. No. 1493, 1932.

29. Pierson, J. Model PBM-3 and 4 Towing Basin Tests to Improve Directional Stability Below Hump Speed. The Glenn L. Martin Company Eng. Report No. 1648, 1942.

30. Pierson, J.D. Directional Stability of Flying Boat Hulls During Taxiing. (Journal of the Aeronautical Sciences, 1944, v. 11, p. 3).

31. Schiff, L.I. and Gimprich, M. Automatic Steering of Ships by Proportional Controls. SNAME Preprint No. 6, May 1949.

32. Schiff, L.I. and Staff of E.T.T., S.I.T. E.T.T., S.I.T. Classified Report No. 288, 1945.

33. Siler, William and Lehman, William. Directional Stability Tests of a Model of the XPBB-1 Flying Boat. E.T.T., S.I.T. Report No. 355, 1948.

34. Strumpf, A. E.T.T., S.I.T. Classified Report No. 327, 1948.

Water Rudders.

35. Abell, T.B. Some Model Experiments on Rudders Placed Behind a Plane Deadwood. I.N.A., 1936.

36. Chillson, C.W. Reversible Pitch Propellers as Applied to Water Handling of Multi-engine Flying Boats. (Journal of the Aeronautical Sciences, v. 7, p. 269, 1940).

37. Darnell, R.C. Hydrodynamic Characteristics of Twelve Symmetrical Hydrofoils. U.S. Experimental Model Basin Report No. 341, 1932.

38. Fischer, K. Calculation of Rudder Force. U.S. Experimental Model Basin Translation No. 52, 1938.

39. Gawn, R.W.L. Steering Experiments. Trans. I.N.A., v.85, 1943.

40. Jones and Cushing. Full Scale Tests of Some Seaplane
        Water Rudders. Marine Aircraft Experimental Estab-
        lishment, Felixstowe, England, 1935.

41. Larsen, Lark. Review of Previously Published Rudder
        Studies. E.T.T., S.I.T. TM No. 79, 1946.

42. Locke, F.W.S., Jr. A Preliminary Correlation of the Be-
        havior of Water Rudders on Seaplanes and Flying Boats.
        NACA T.N. No. 1387, 1947.

42a. Pfingstag, H.T. and Sprenger, F.C. Investigation of Rud-
        der Action by Wind Tunnel Experiments. Thesis, Massa-
        chusetts Institute of Technology, 1932.

43. Pitre, A.S. and Thews, J.G. Comparative Rudder Tests -
        Model and Full Scale. U.S.E.M.B. Report No. 397.

44. Schoenherr, Karl E. Steering. Principles of Naval Archi-
        tecture, v. II. S.N.A.M.E., New York, 1941.

Low Aspect Ratio Lift Theory.

45. Bollay, William. A Non-linear Wing Theory and Its Appli-
        cations to Rectangular Wings of Small AR. Z.f.a.M.M.,
        Bd. 19, Heft 1, Feb. 1939, pp. 21-35.

46. Diederich, F.W. and Zlotnick, M. Theoretical Spanwise
        Lift Distributions of Low-Aspect Ratio Wings at Speeds
        Below and Above the Speed of Sound. NACA T.N. No. 1973,
        1949.

47. Diehl, W.S. Variation of Lift and Drag Coefficients with
        Changes in Size and Speed. NACA Annual Report t, 1921.

48. Diehl, W.S. Effect of Airfoil Aspect Ratio on the Slope
        of the Lift Curve. NACA T.N. No. 79, 1922.

49. Higgins, G. The Prediction of Airfoil Characteristics.
        NACA Report No. 312.

50. Jones, R.T. Properties of Low-Aspect Ratio Pointed Wings
        at Speeds Above and Below the Speed of Sound. NACA
        T.N. No. 1032, 1946.

51. Jacobs, E.N. and Anderson, R.F. Large-Scale Aerodynamic
        Characteristics of Airfoils. NACA Report No. 352, 1930.

52. Jacobs.   Tests of Six Symmetrical Airfoils in the Variable
     Density Wind-Tunnel.   NACA T.N. No. 385, 1931.

53. Locke, F.W.S., Jr.   An Empirical Study of Low Aspect Ratio
     Lifting Surfaces with Particular Regard to Planing
     Craft.   (Journal of the Aeronautical Sciences, 1949,
     v. 16, p. 184).

54. Milne-Thomson.   Theoretical Aerodynamics.

55. von Mises, Richard.   Theory of Flight.   New York, McGraw
     Hill, 1945.

56. Siler, William.   Lift and Moment of Low Aspect Ratio Rec-
     tangular Lifting Surfaces.   Master's Thesis.   S.I.T.,
     Hoboken, 1949.

57. Weinig.   Lift and Drag of Wings with Small Span.   NACA
     T.M. 1151, 1947.

58. Winter, H.   Flow Phenomena on Plates and Airfoils of Short
     Span.   Verein Deutscher Ingenieure.   Special Issue
     (Aviation), 1936.   Trans.: NACA T.M. No. 798, 1936.

59. Wood, K.D.   Technical Aerodynamics.   Ithaca, N.Y., Cornell
     Co-op Society, 1934.

60. Zimmerman.   Characteristics of Clark Airfoils of Small
     Aspect Ratios.   NACA Report No. 431.

TABLE I

SPEED RELATIONSHIPS

Spd. No.	V_m		V_m^2	qS	C_V	V_s
	ft./sec.	knots	ft.^{2}/sec.^{2}	lb.		kts.
L-9	1.9970	1.182	3.988	.0268	0.521	5.55
L-17	3.0560	1.810	9.32	.0628	0.798	8.50
L-24	3.9836	2.360	15.89	.1070	1.041	11.10
H_1-11	6.1210	3.622	37.48	.2524	1.600	17.03

Plotting
Code

	Aspect Ratio, A		
	0.5	1.0	2.0
C_V 0.521	⌐	⊔	⊏
0.798	⊐	⊡	⊏
1.041	⌐	⊓	⌐
1.600	▽	▽	▽

TABLE II

EFFECTIVE ASPECT RATIO

Formula (Ref. 59):

$$\frac{dC_L}{d\alpha} = \frac{0.1}{1 + 2/A_e} \qquad \text{or} \qquad A_e = \frac{2}{\dfrac{1}{10\dfrac{dC_L}{d\alpha}} - 1}$$

	A = 0.5		A = 1.0		A = 2.0	
C_v	$\frac{dC_L}{d\alpha}$	A_e	$\frac{dC_L}{d\alpha}$	A_e	$\frac{dC_L}{d\alpha}$	A_e
0.521	.0250	0.665	.0470	1.750	.0500	2.000
0.798	.0247	0.650	.0415	1.400	.0470	1.750
1.041	.0242	0.630	.0362	1.140.	.0530	2.245
1.600	.0239	0.620	.0348	1.065	.0480	1.730
Averages						
0.990	.0244	0.641	.0399	1.339	.0495	1.931
Gain		+28%		+20%		-2.6%

TABLE IIIa

α_H	ψ_T	$(C_{M_\psi})_T$	$(C_L)_R$	α
-2	-.05	-.00121	-.0935	-1.95
+8	+.15	+.00362	+.280	+7.85
23	.30	.00725	.560	22.7
28	.35	.00845	.655	27.65
31	.40	.00966	.748	30.6
33	.45	.0109	.841	32.55
38	.45	.0109	.841	37.55
43	.40	.00966	.748	42.6
48	.35	.00845	.655	47.65

Cv: 0.5-1   A 1.0

α	ψ	(c_ψ)	(c_L)	α
-2	-.05	-.00121	-.0935	-1.95
+3	+.10	+.0022	+.374	+2.90
6	.20	.00424	.374	5.80
8	.25	.00604	.467	7.75
13	.35	.00848	.655	12.65
15.5	.35	.00845	.655	15.15
18	.45	.0109	.841	17.55
19	.40	.00966	.743	18.60
21	.45	.0109	.841	20.55
22	.45	.0109	.841	21.55
23	.50	.0121	.935	22.60
24	.50	.0121	.935	23.60
25	.45	.0109	.841	24.55
26	.45	.0109	.841	25.55
28	.45	.0109	.841	27.55
34	.45	.0109	.841	33.55
38	.45	.0109	.841	37.55

TABLE IIIc

TABLE IIIc

C_V: 0.521 A: 2.0

α_H	ψ_T	$(C_{M_\psi})_T$	$(C_L)_R$	α
-4	-.1	-.00242	-.187	-3.9
+1	+.05	+.00121	+.0935	+.95
6	.15	.00362	.280	4.85
11	.225	.00544	.421	10.8
16	.30	.00725	.560	15.7
21	.30	.00725	.560	20.7
26	.30	.00725	.560	25.7
31	.30	.00725	.560	30.7
36	.275	.00665	.514	35.7
46	.25	.00604	.467	45.75

TABLE IVa

A: 0.5

α_H	ψ_T	$(C_{M_\psi})_T$	$(C_L)_R$	α
-4	-.1	-.00242	-.0678	-3.9
+3	+.15	+.00362	+.102	+2.85
8	.25	.00604	.169	7.75
13	.50	.0121	.339	12.5
18	.70	.0169	.475	17.3
23	.90	.0217	.610	22.1
28	1.05	.0254	.711	26.95
33	1.2	.0290	.814	31.8
38	1.3	.0314	.881	36.7
40	1.35	.0326	.915	38.65
42	1.4	.0338	.950	40.6
43	1.4	.0338	.950	41.6
44	1.3	.0314	.881	42.7
48	1.15	.0278	.780	46.85
53	1.1	.0266	.745	51.9

TABLE IVb

α_H	ψ_T	$(C_{M_\psi})_T$	$(C_L)_R$	α
-2	-.15	-.00362	-.102	-1.85
+3	+.20	+.00484	+.136	+2.80
13	.75	.0181	.508	12.25
17	1.00	.0242	.678	16.00
18	.95	.0229	.644	17.05
19	1.15	.0278	.780	17.85
20	1.10	.0266	.745	18.90
21	1.10	.0266	.745	19.90
23	1.10	.0266	.745	21.90
28	1.10	.0266	.745	26.90
31	1.10	.0266	.745	29.90
33	1.05	.0254	.712	31.95
43	.90	.0217	.641	42.10

TABLE IVc

α_H	ψ_T	$(C_{M_\psi})_T$	$(C_L)_R$	α
−4	−.25	−.00604	−.169	−3.75
+1	+.10	+.00242	+.0678	+.90
3.5	.20	.00484	.136	3.30
6	.40	.00966	.271	5.60
8.5	.65	.0157	.440	7.85
11	.85	.0205	.576	10.15
16	1.10	.0266	.745	14.90
19	1.05	.0254	.712	17.95
21	1.20	.0290	.814	19.80
23	1.20	.0290	.814	21.80
25	1.25	.0302	.847	23.75
26	1.25	.0302	.847	24.75
27	1.20	.0290	.814	25.80
28	1.20	.0290	.814	26.80
29	1.20	.0290	.814	27.80
30	1.15	.0278	.780	28.85
31	1.10	.0266	.745	29.90
36	1.05	.0254	.712	34.95
46	1.00	.0242	.678	45.00

C_V: 1.041   A: 0.5

α_H	ψ_T	$(C_{M_\psi})_T$	$(C_L)_R$	α
-2	-.05	-.00121	-.0131	-1.95
+3	+.40	+.00966	+.1045	+2.60
6	.80	.0193	.209	5.20
8	1.00	.0242	.261	7.00
13	1.40	.0338	.366	11.60
18	1.80	.0435	.470	16.20
23	2.15	.0520	.561	20.85
28	2.60	.0629	.679	25.40
33	3.00	.0725	.784	30.00
37	3.30	.0798	.861	33.70
41	3.70	.0895	.965	37.30
43	4.60	.0111	1.200	38.40
44	3.80	.0919	.991	40.20
45	3.80	.0919	.991	41.20
46	3.60	.0870	.940	42.40
47	2.80	.0676	.731	44.20
48	2.75	.0665	.718	45.25
50	.50	.0121	.131	49.50
53	2.50	.0604	.652	50.50

TABLE Vb

<u>Cy: 1.041</u>   <u>A: 1.0</u>

α_H	ψ_T	$(C_{M_\psi})_T$	$(C_L)_R$	α
-2	-.20	-.00484	-.0522	-1.80
+3	+.40	+.00966	+.1046	+2.60
8	1.15	.0278	.3001	6.85
13	1.40	.0338	.366	11.60
16	2.00	.0484	.522	14.00
18	2.40	.0580	.626	15.60
21	2.50	.0604	.652	18.50
23	2.35	.0689	.745	20.15
24	2.70	.0652	.705	21.30
26	2.30	.0676	.731	23.40
27	2.30	.0676	.731	24.20
27.5	2.75	.0665	.718	24.75
28	2.35	.0689	.745	25.15
28.5	2.55	.0616	.665	25.95
29	2.50	.0604	.652	26.50
30	2.50	.0604	.652	27.50
31	2.25	.0544	.587	28.75
33	2.45	.0592	.640	30.55
35	2.30	.0555	.600	32.70
38	2.30	.0555	.600	35.70

TABLE V**c**

C_V: 1.041   A: 2.0

α_H	ψ_T	$(C_{M_\psi})_T$	$(C_L)_R$	α
-4	-.60	-.0145	-. 157	-3.40
-1.5	-.20	-.00484	-.0522	-1.30
+1	+.20	+.00484	+.0522	+ .80
4	.65	.0157	.170	3.35
8	1.55	.0374	.405	6.45
11	1.95	.0471	.509	9.05
14	2.40	.0580	.626	11.60
16	2.75	.0665	.718	13.25
19	2.95	.0713	.770	16.05
21	3.00	.0725	.784	18.00
22	3.15	.0761	.822	18.85
23	3.20	.0775	.835	19.80
24	3.15	.0761	.822	20.85
25	3.25	.0785	.849	21.75
26	3.10	.0750	.810	22.90
27	3.20	.0774	.835	24.80
28	3.00	.0725	.784	25.00
29	3.00	.0725	.784	26.00
30	2.75	.0665	.718	27.25
31	2.70	.0652	.705	28.30
33	2.60	.0628	.679	30.40

TABLE Vc   (cont.)

C_V: 1.041   A: 2.0

α_H	ψ_T	$(C_{M_\psi})_T$	$(C_L)_R$	α
36	2.40	.0530	.626	33.60
41	2.30	.0555	.600	38.70
46	2.20	.0531	.575	43.80

C_V: 1.600 $\qquad\qquad\qquad\qquad\qquad\qquad\qquad$ A: 0.5

α_H	ψ_T	$(C_{M_\psi})_T$	$(C_L)_R$	α
-2	-.30	-.00725	-.0388	-1.70
+3	+.40	+.00966	+.0518	+2.60
8	1.15	.0278	.149	6.85
13	1.80	.0435	.233	11.20
18	2.65	.0640	.343	15.35
23	2.65	.0640	.343	20.35
28	4.45	.1075	.575	23.55
33	5.20	.1258	.673	27.80
38	5.90	.1426	.764	32.10
43	6.20	.1500	.802	36.80
45	6.45	.1560	.835	38.55
47	6.85	.1655	.886	40.15
48	6.80*	1.5700*	.840*	41.50*
49	7.20	.1740	.931	41.80
50	5.50*	.1330*	.711*	44.50*
53	5.00*	.1210*	.647*	48.00*

* Oscillating

52

Cv: 1.600   A: 1.0

$\propto_H$	ψ_T	$(C_{M_\psi})_T$	$(C_L)_R$	$\propto$
-2	-.15	-.00362	-.0194	-1.85
+3	+.80	+.0193	+.104	+2.2
11	2.40	.0580	.310	8.6
19	4.25	.1027	.550	14.75
23	5.10	.1230	.660	17.9
26	5.40	.1303	.699	20.6
28	5.50	.1330	.711	22.5
29	5.40	.1303	.699	23.6
30	5.60	.1351	.725	24.4
31	5.30	.1280	.685	25.7
32	5.00	.1210	.647	27.0
33	5.00	.1210	.647	28.0
34	4.80	.1160	.621	29.2
35	4.70	.1136	.608	30.3
38	4.70	.1136	.608	33.3
43	4.40	.1062	.570	38.6

TABLE VIc

α_H	ψ_T	$(C_{M_\psi})_T$	$(C_L)_R$	α
-4	-.95	-.0230	-.123	-3.05
+1	+.40	+.0097	+.052	+0.60
11	3.15	.0760	.408	7.85
19	5.25	.1270	.680	13.75
20	5.45	.1317	.705	14.55
21	5.85	.1412	.757	15.15
22	5.90	.1425	.764	16.10
23	5.95	.1438	.770	17.05
24	6.00	.1450	.776	18.00
24.5	5.95	.1438	.770	18.55
25	5.85	.1412	.757	19.15
26	5.85	.1412	.757	20.15
27	5.70	.1378	.738	21.30
28	5.70	.1378	.738	22.30
29	5.50	.1330	.711	23.50
30	5.50	.1330	.711	24.50
31	5.45	.1317	.705	25.55
34	5.20	.1256	.673	28.80
38	5.00	.1210	.647	33.00
46	4.75	.1148	.615	41.25
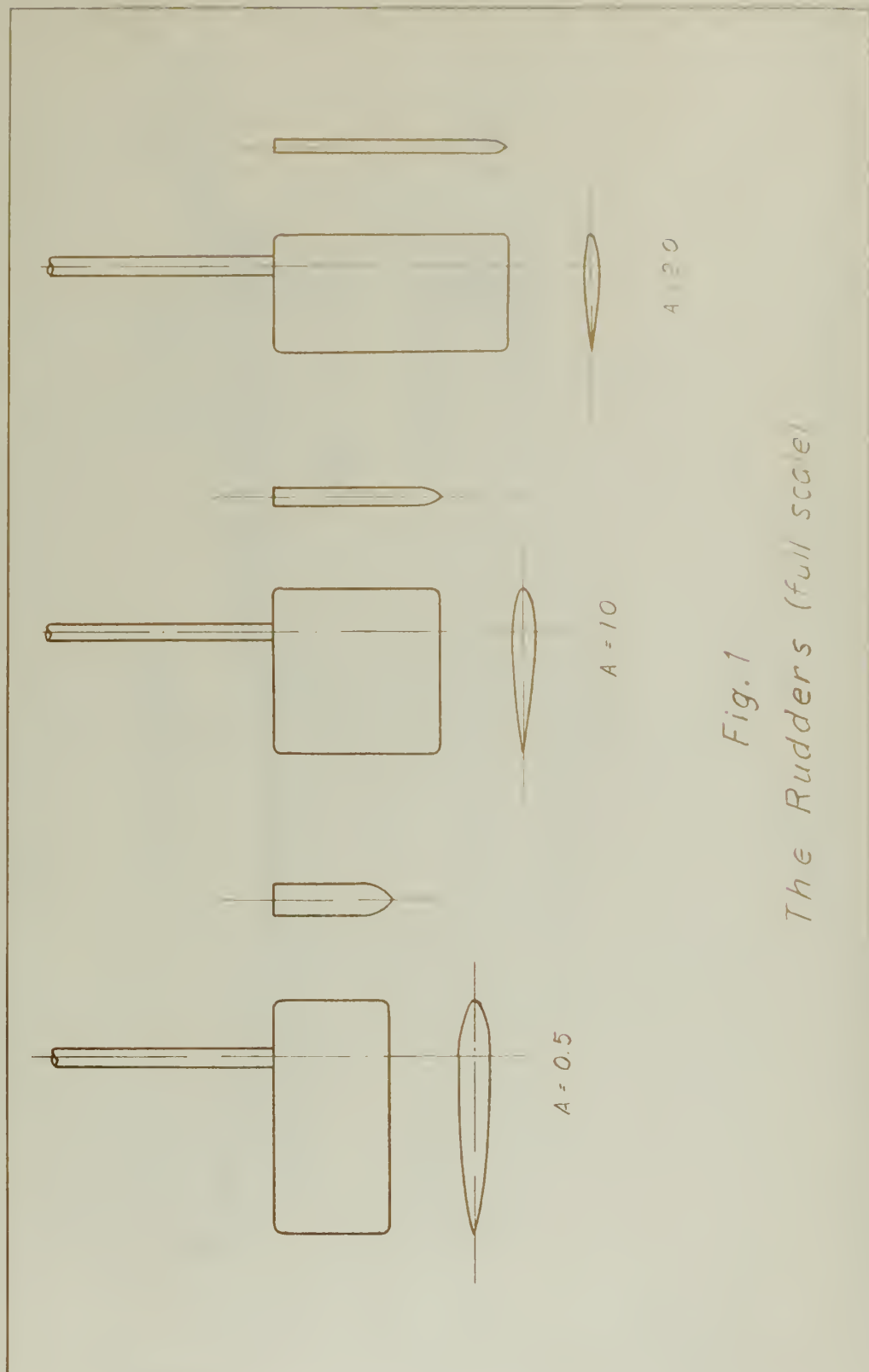
Fig. 1

The Rudders (full scale)

15 in.

13 in.

c.g.
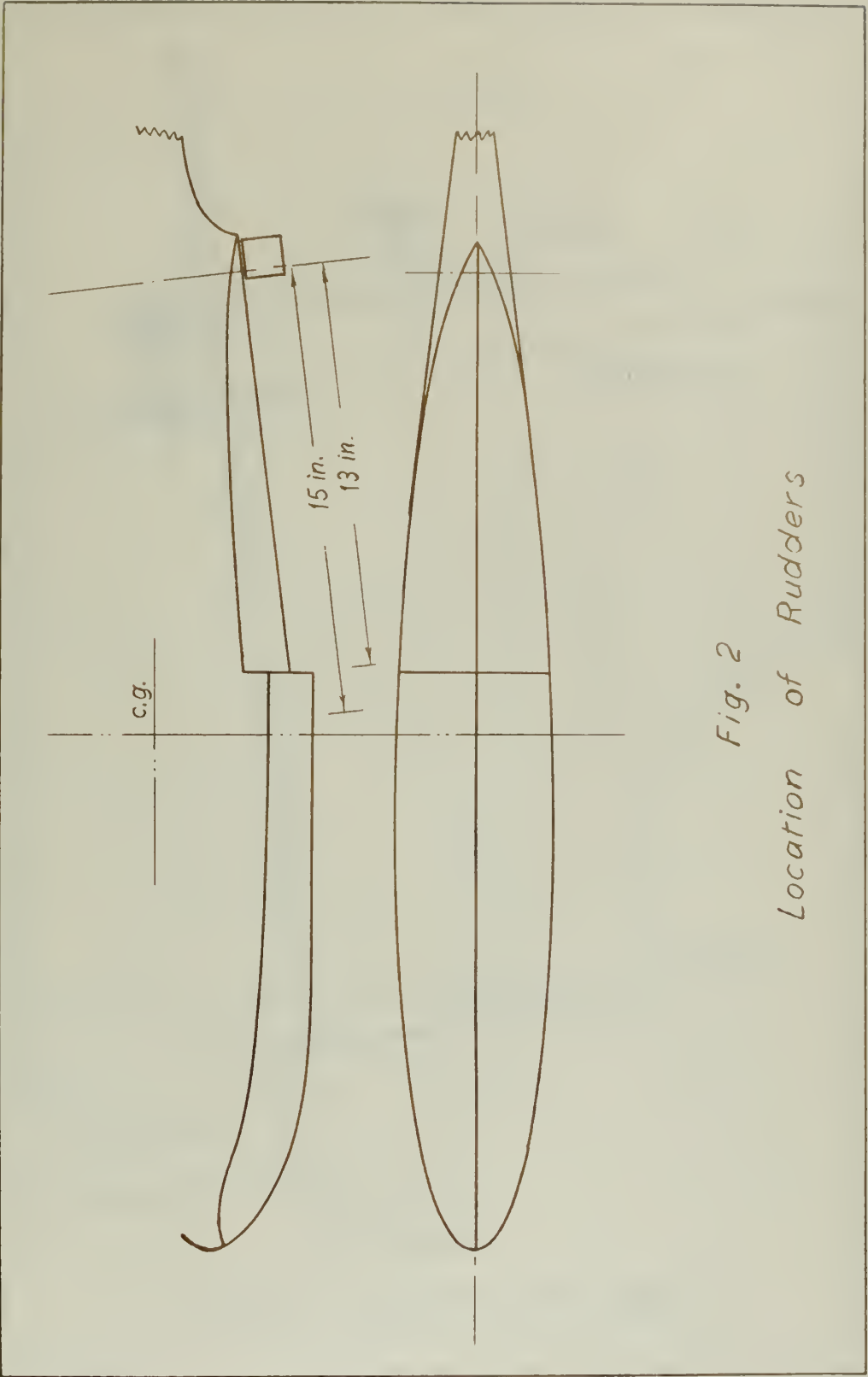
Fig. 2   Location of Rudders

Pointer

Protractor

Model deck

Sternpost

13 in. to step

15 in. to c.g.

Fig. 2a

Rudder Installation (full scale)
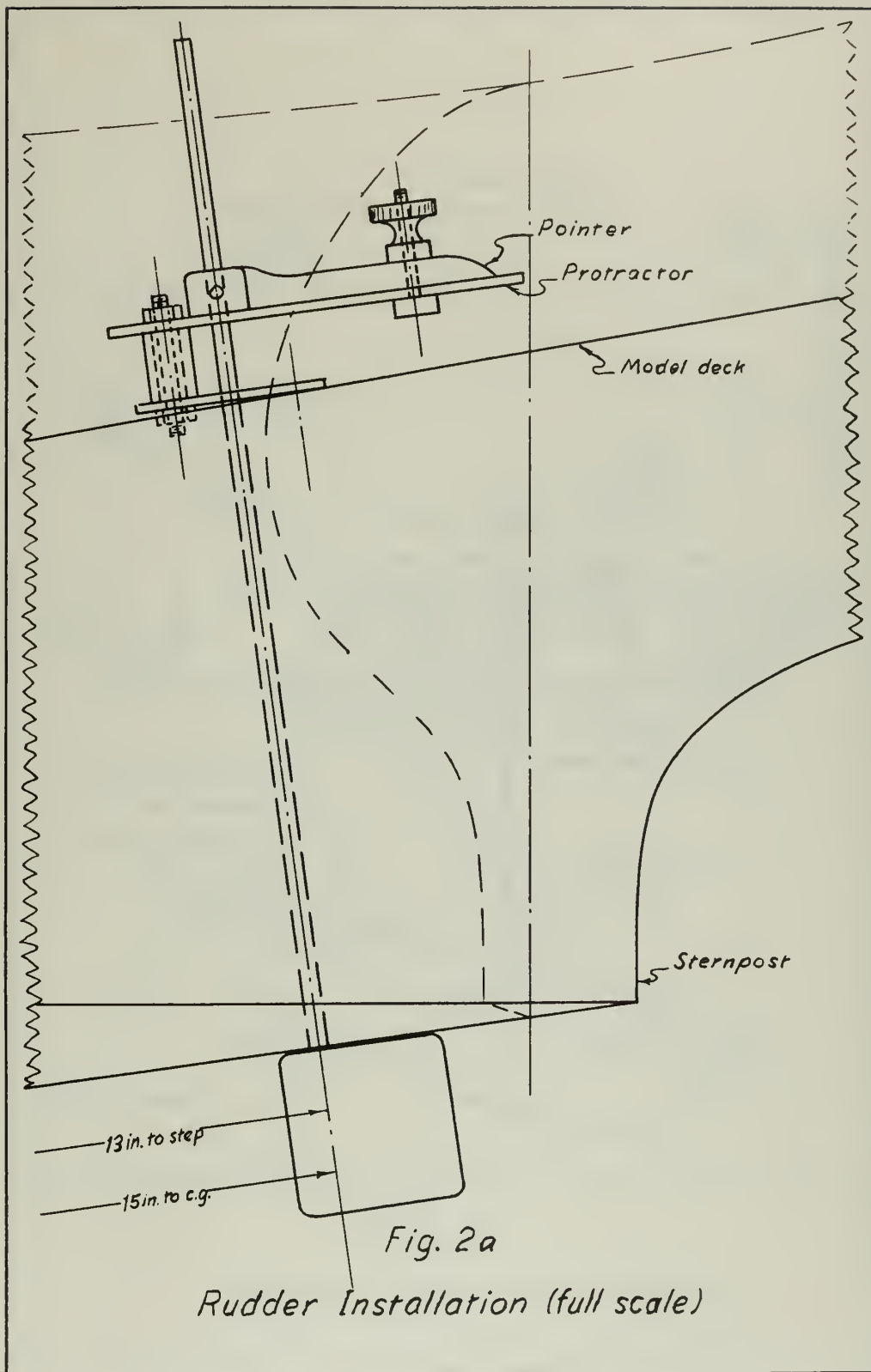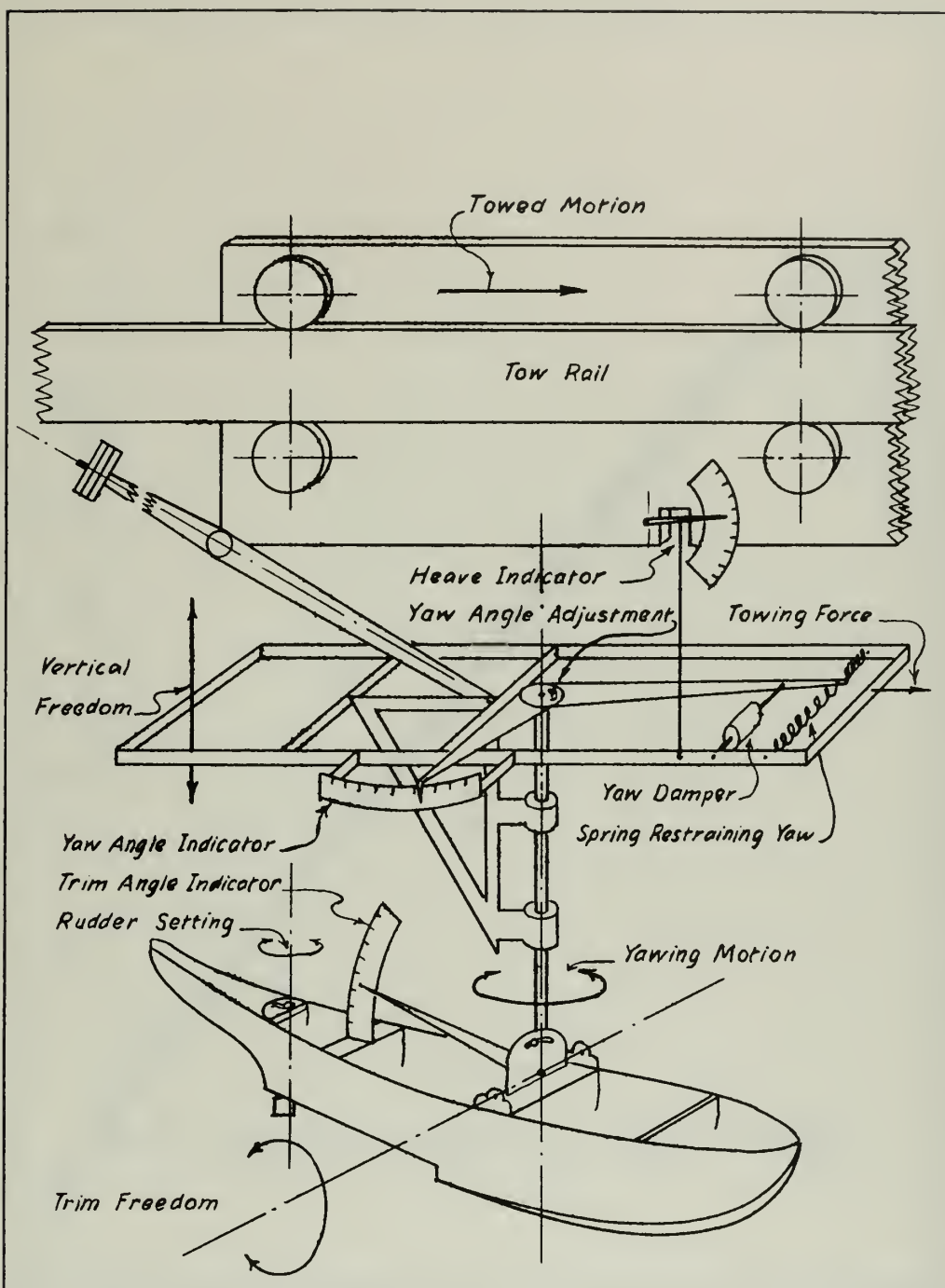
Fig. 3

Yawing Apparatus (Schematic)
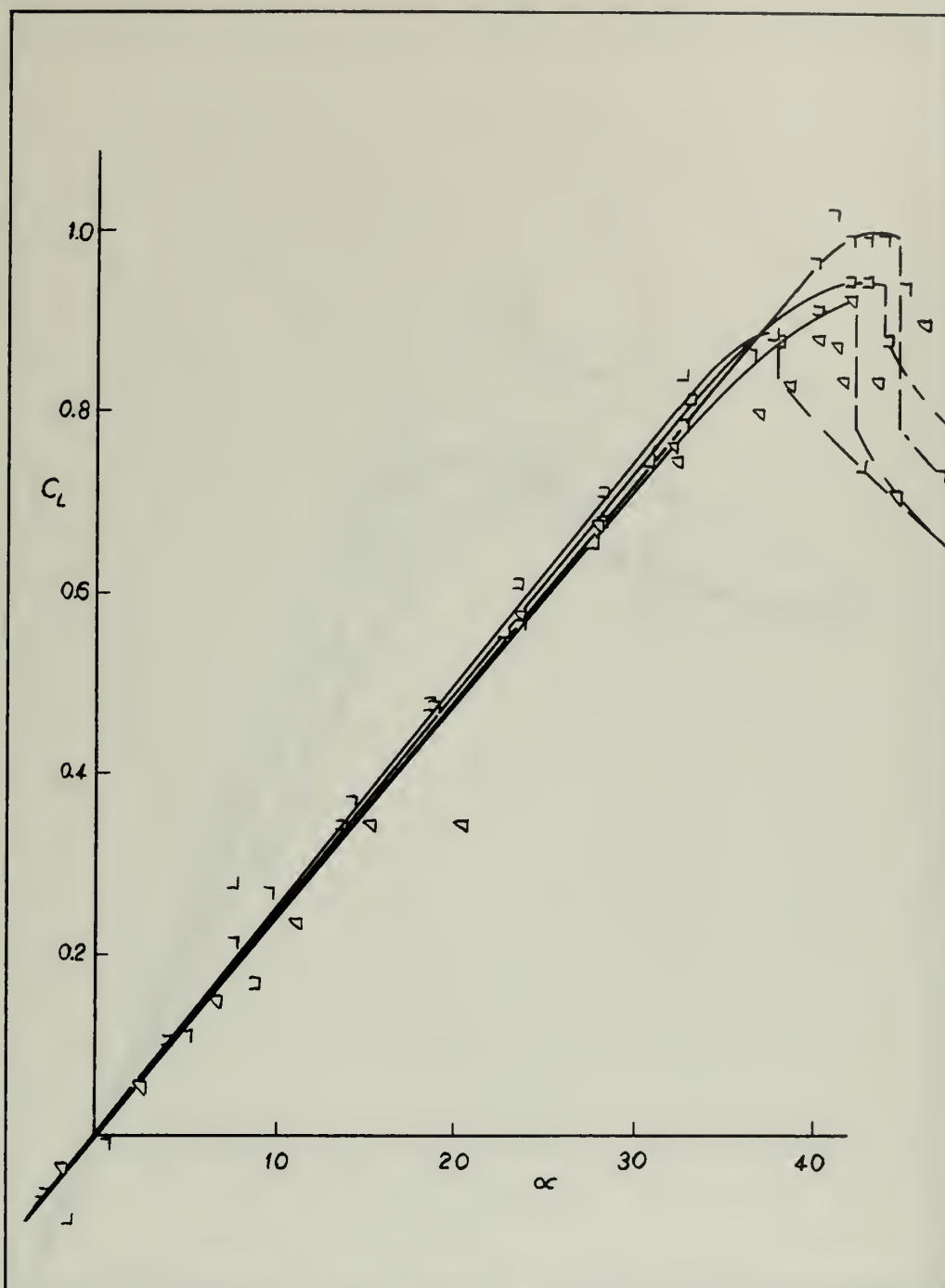
Fig. 4

Lift Curve for A = 0.5
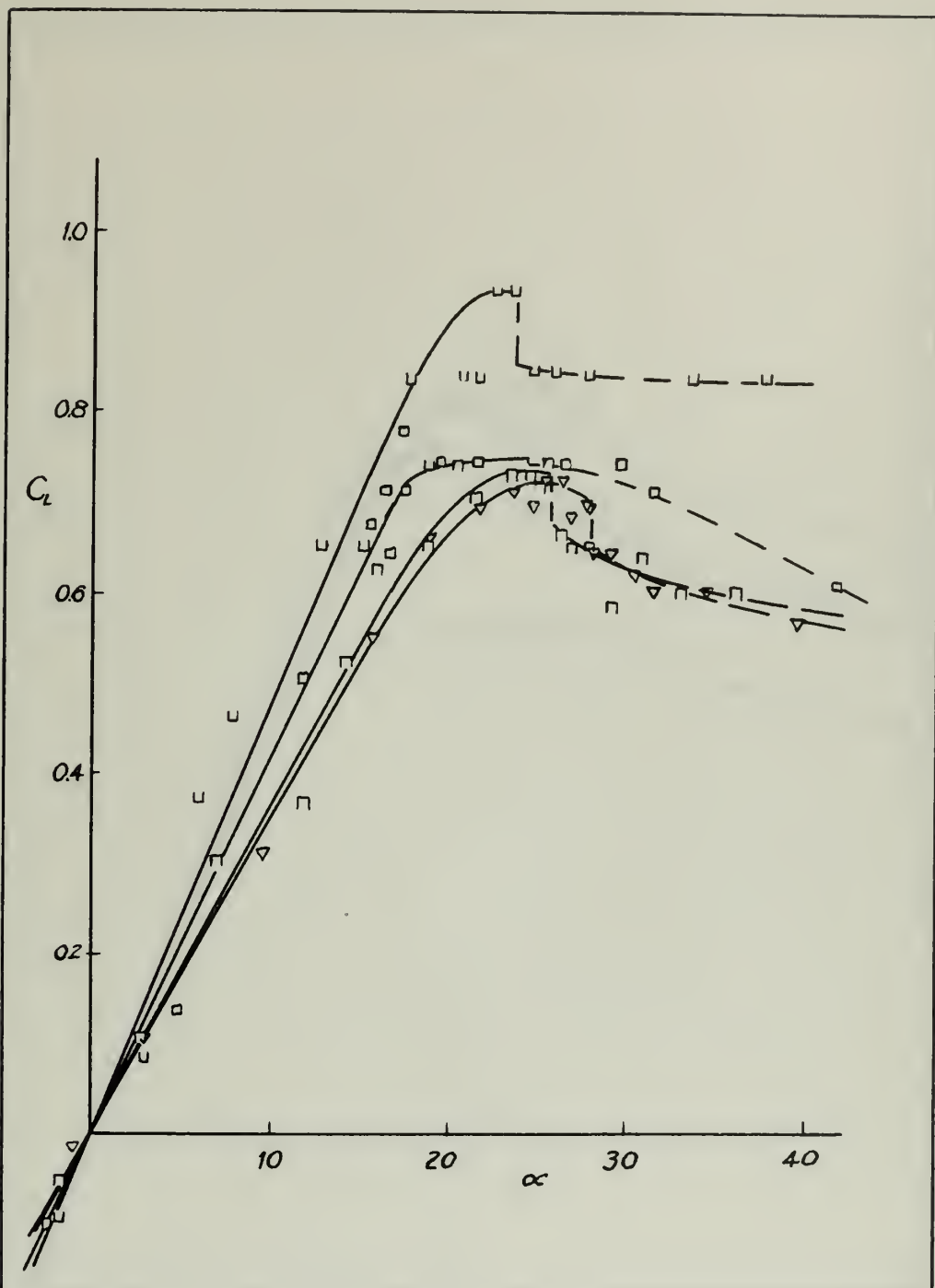
Fig. 5

Lift Curve for A = 1.0
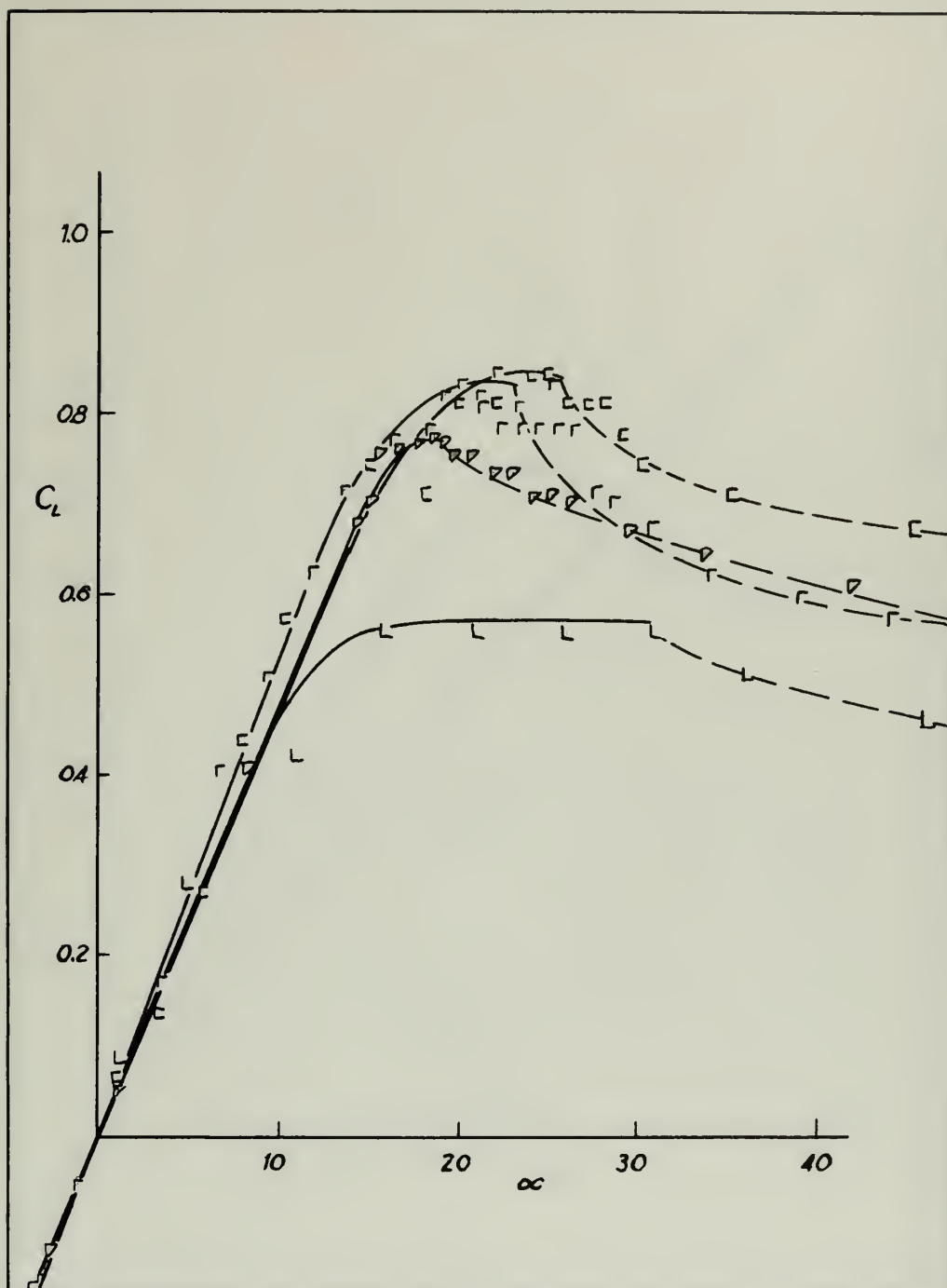
Fig. 6

Lift Curve for A = 2.0
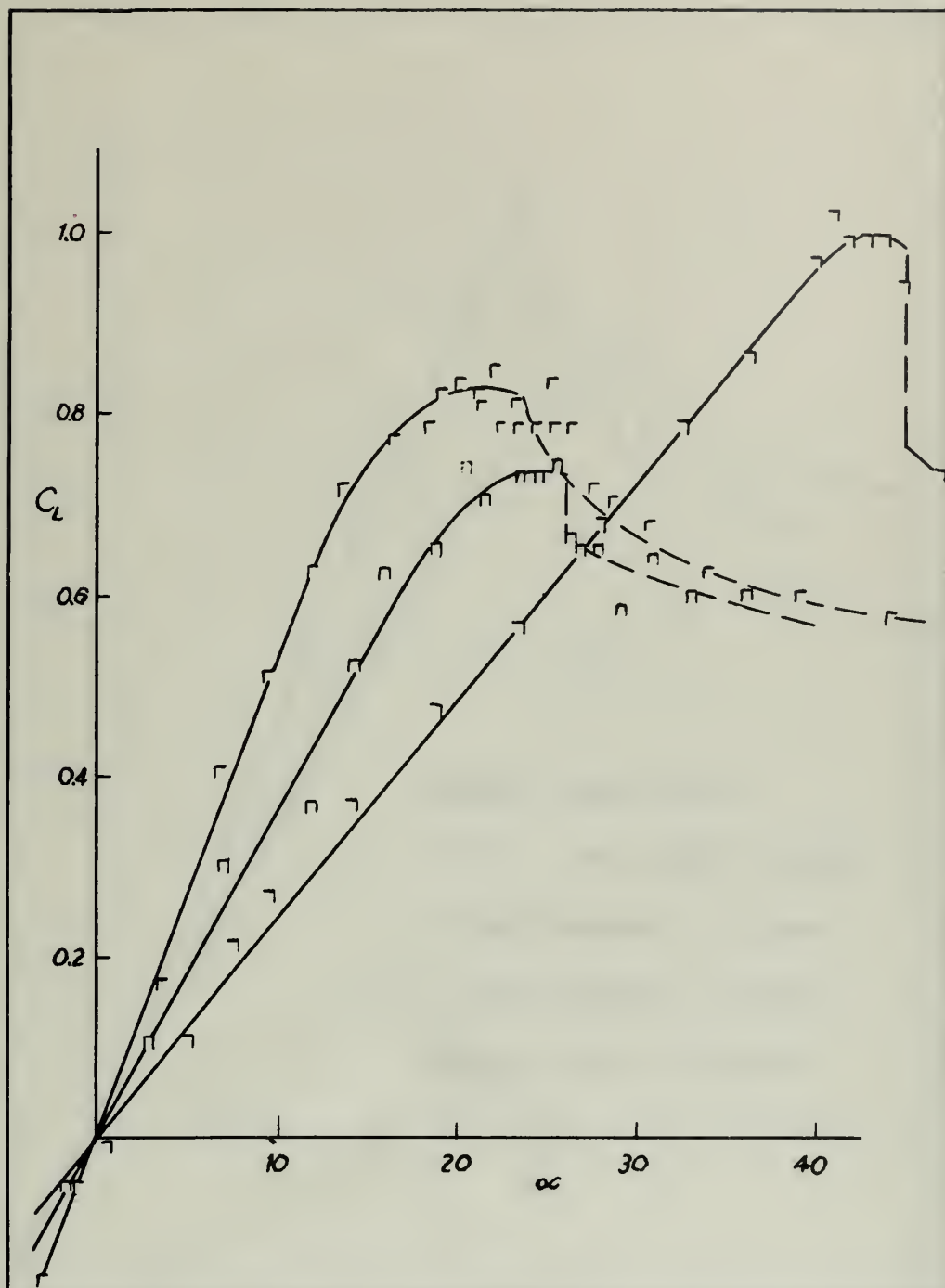
Fig. 7

Aspect Ratio Effects ($C_v = 1.041$)

62

Darnall Rudder Data:

A = 1.0   t/c = 0.128 V_m = 2.5 kts.

⊙ Hull clearance: 0 span

✗ Hull clearance: 1/3 span

Rudder under flat bottom.
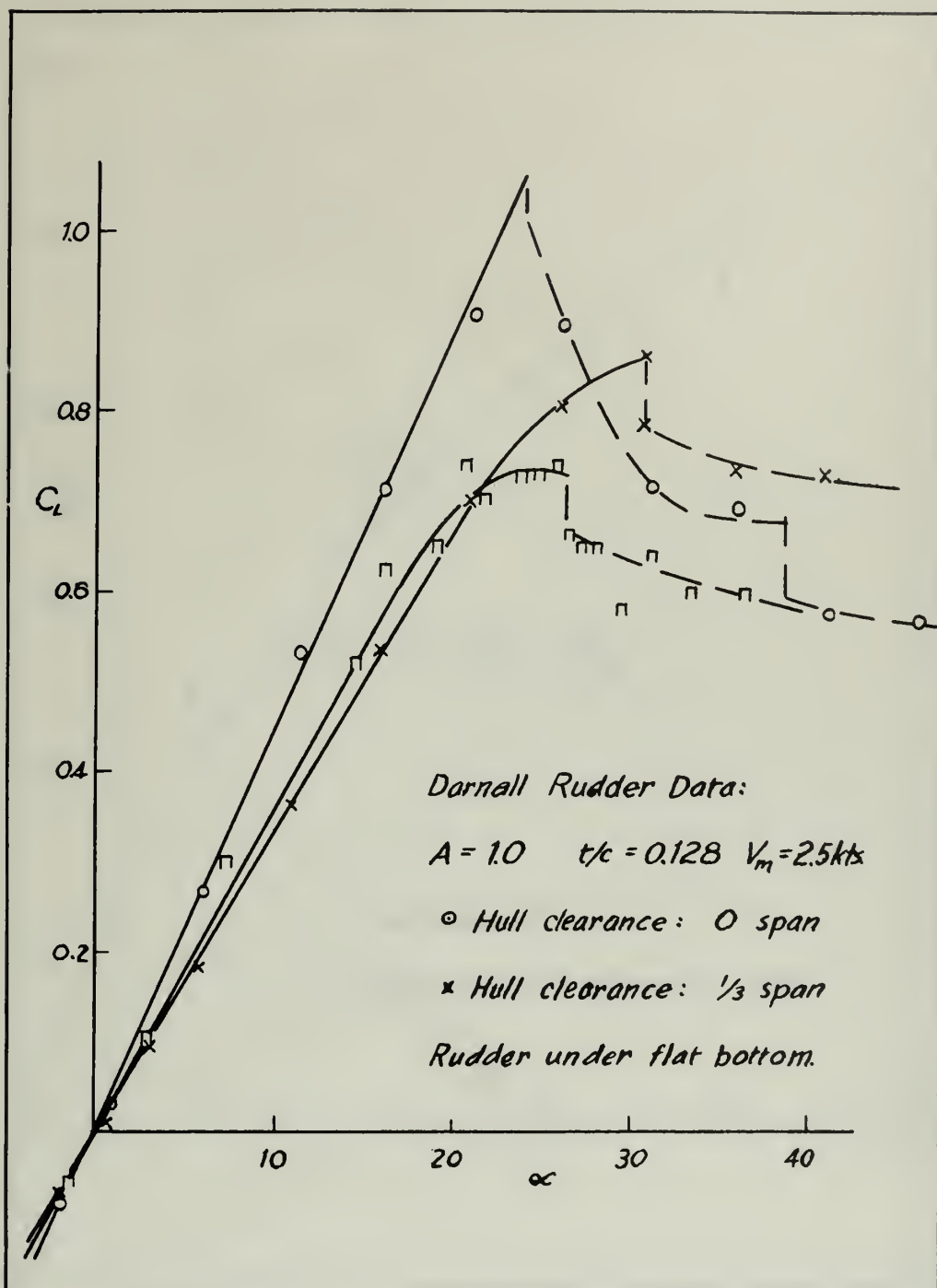
Fig. 8

Gap Effects. Rough Comparison with Darnell [37]

63

$$\frac{dC_L}{d\alpha} = \frac{0.1}{1 + \frac{2}{A}}$$

⊙ From Dornell (37)

✦ From M.I.T. Rudder Investigation (42A)
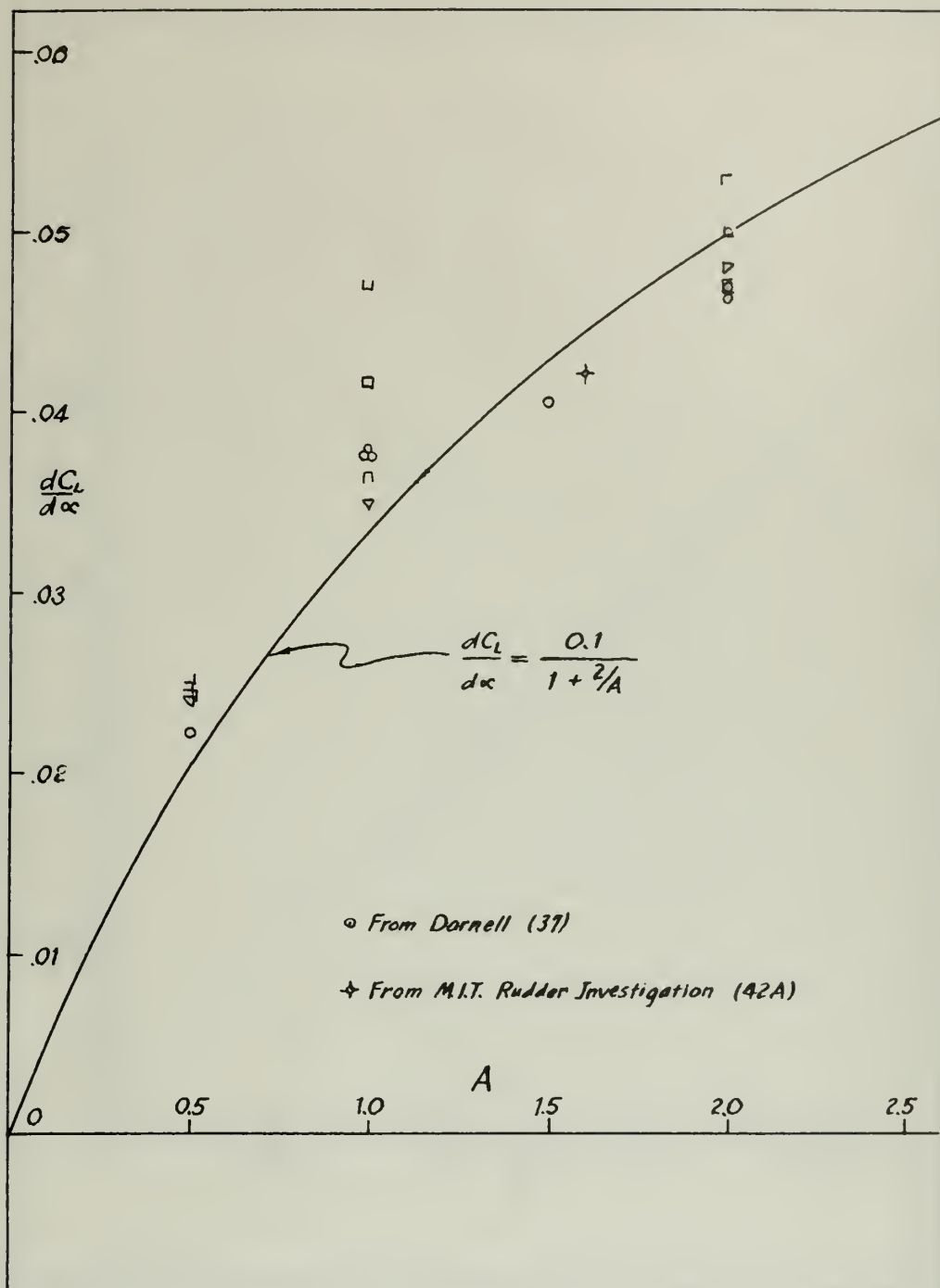
Fig. 9

Relation of Lift-curve Slope to Aspect Ratio.
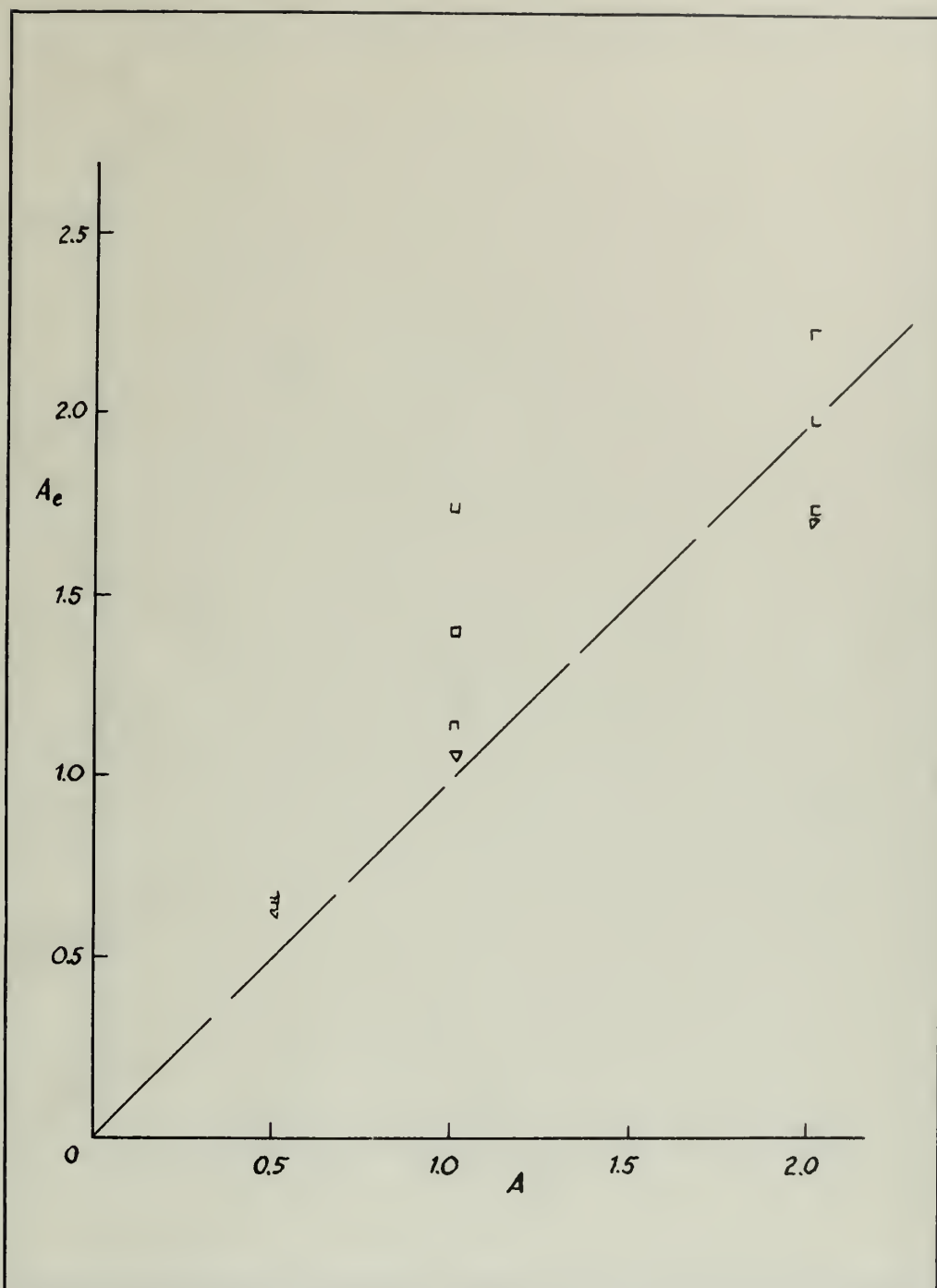
Fig. 10

Relation of Effective to Actual Aspect Ratio.
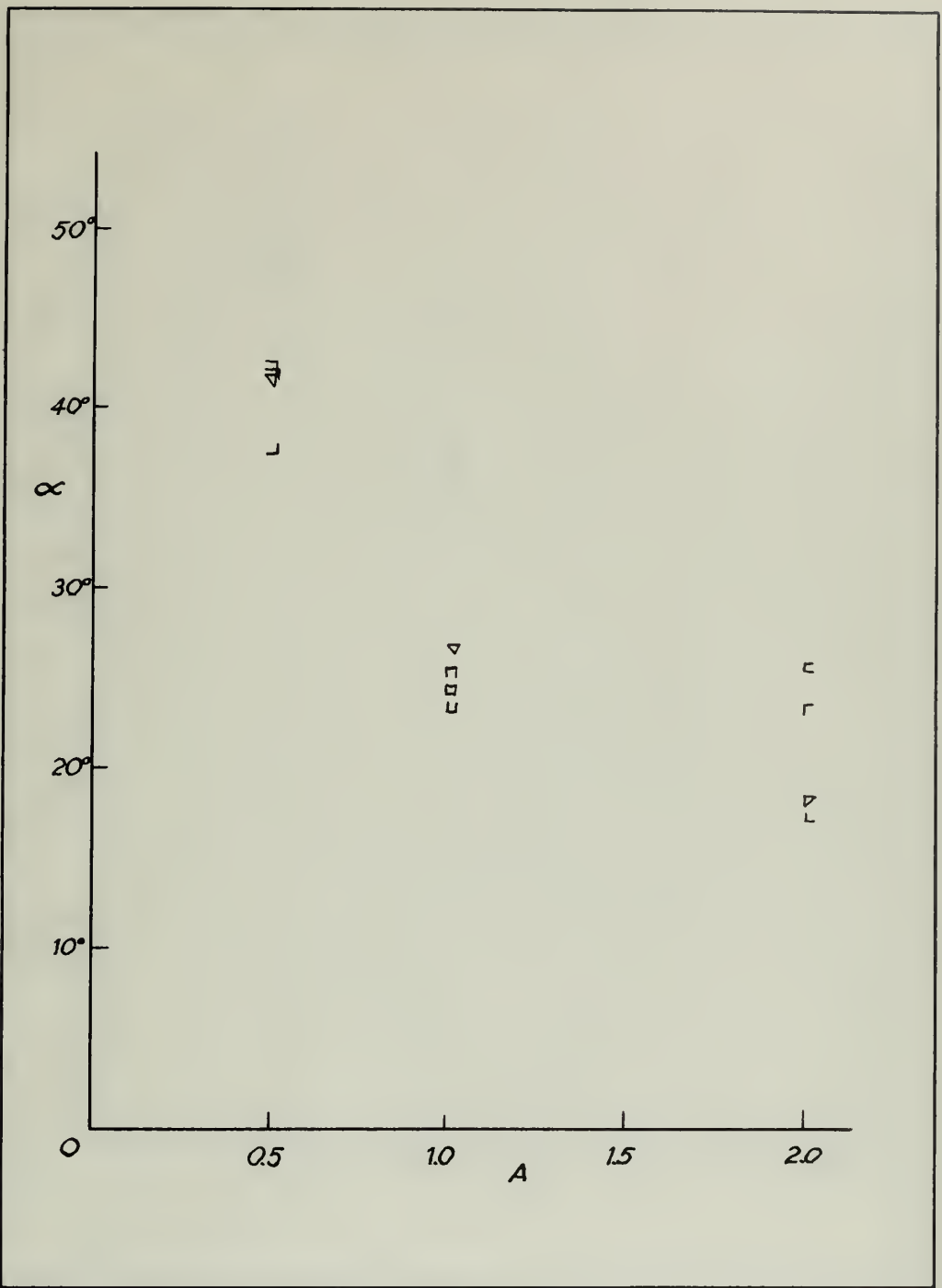
Fig. 11

Relation of Burble Point and Aspect Ratio
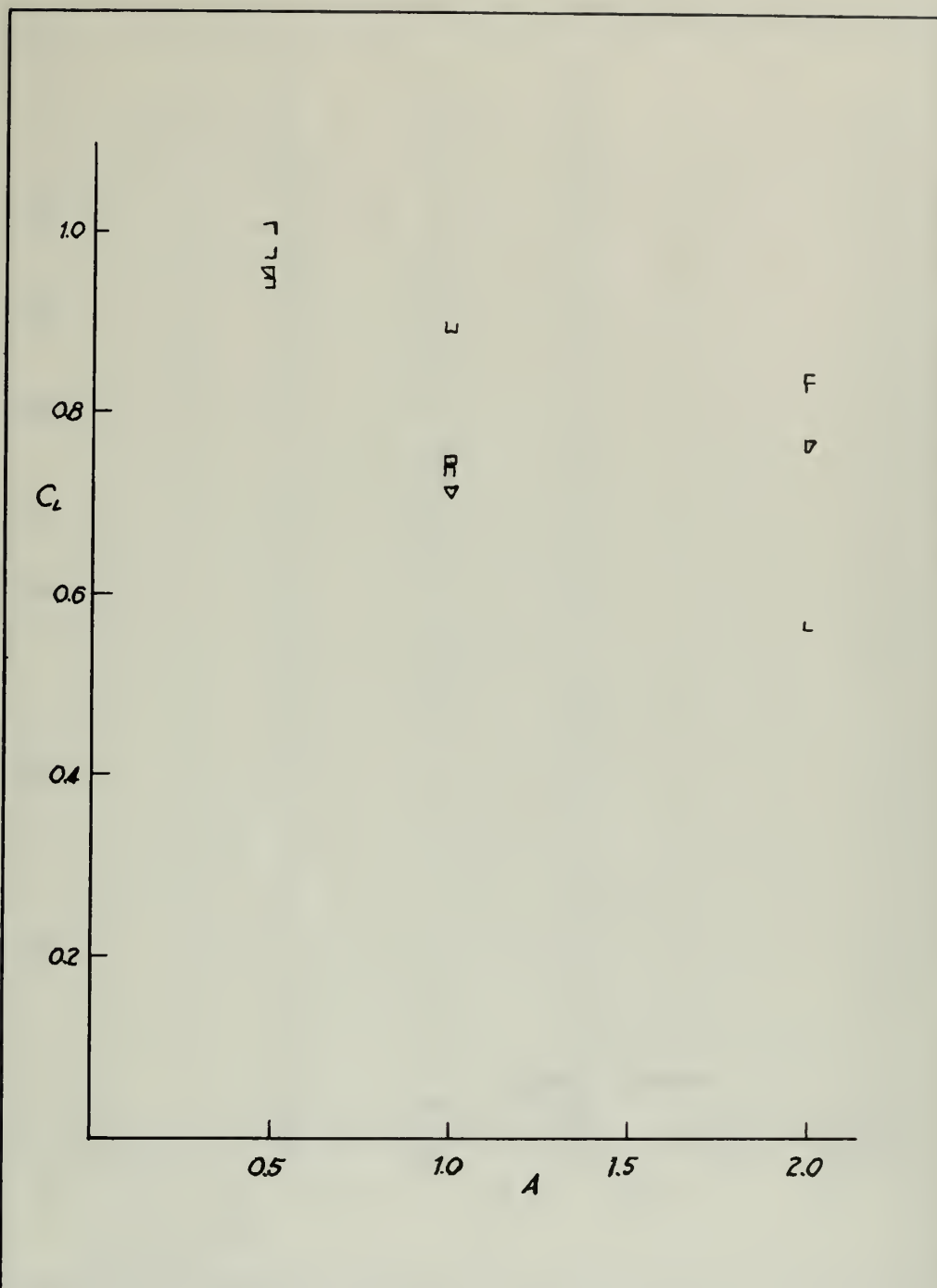
Fig. 12

Relation of Maximum Lift and Aspect Ratio
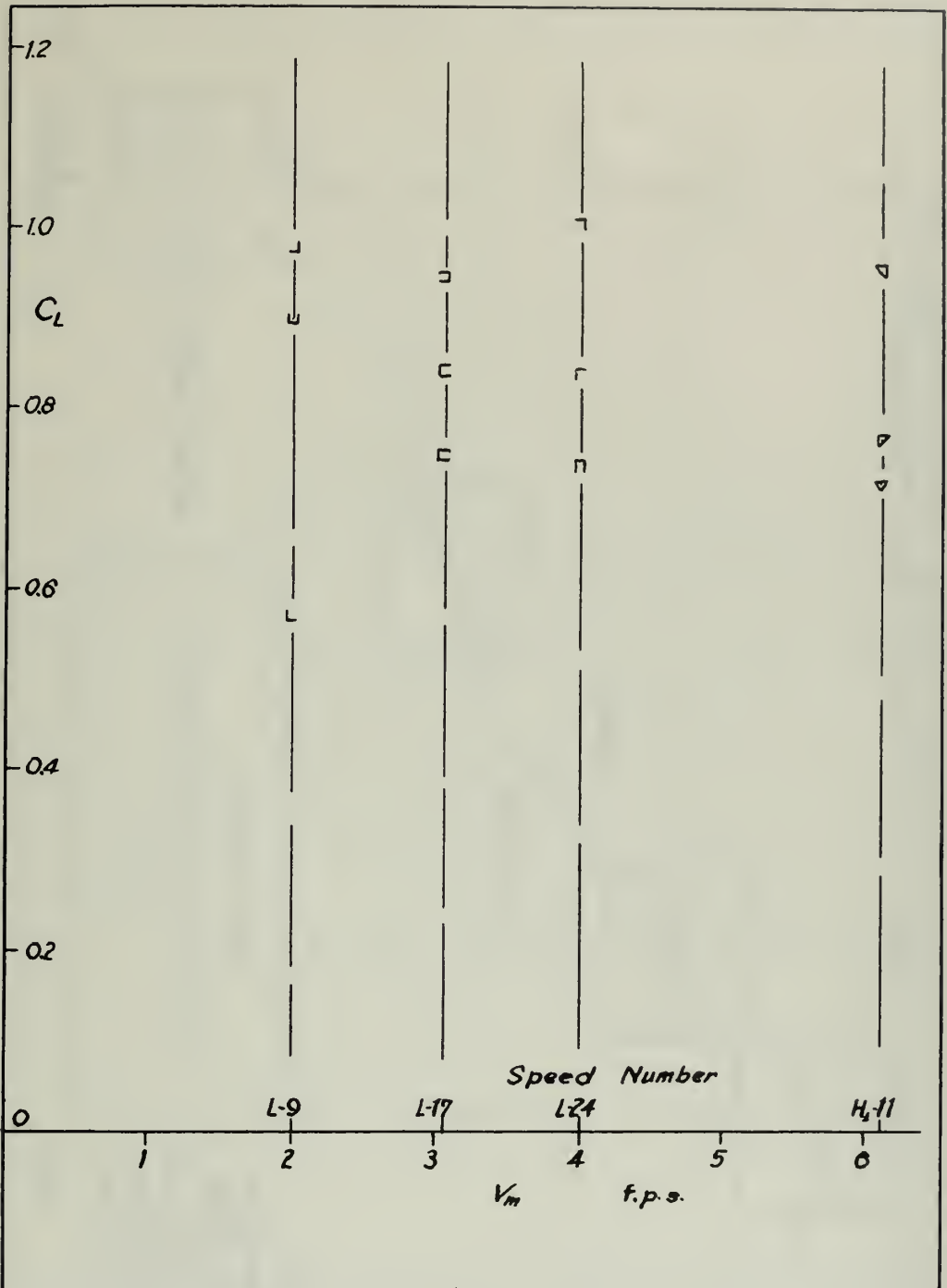
Fig. 13

Relation of Maximum Lift and Speed

Fig. 14
Directional Characteristics
(Hull Alone)

Fig. 15

Yawing Curves, With and Without Rudder
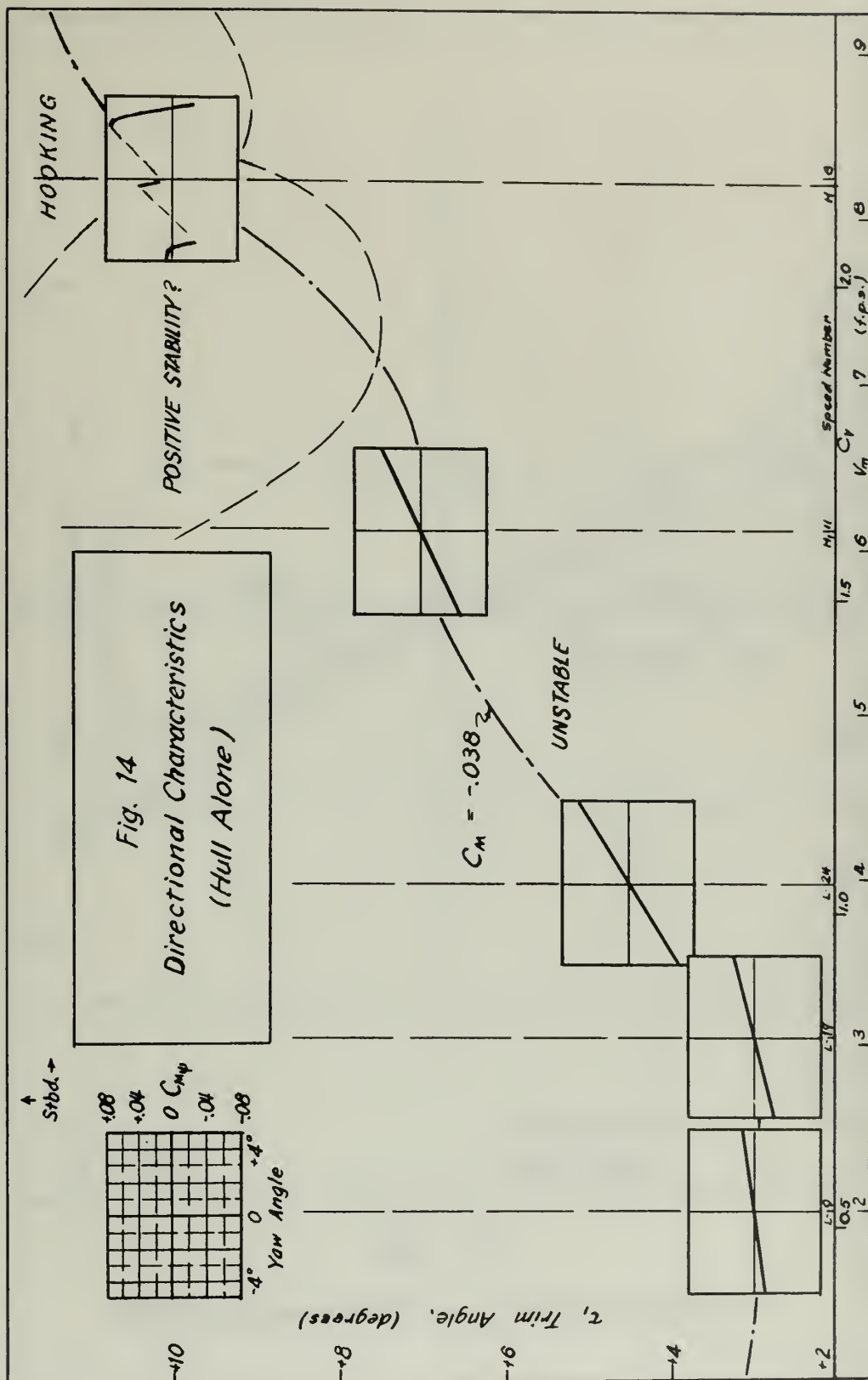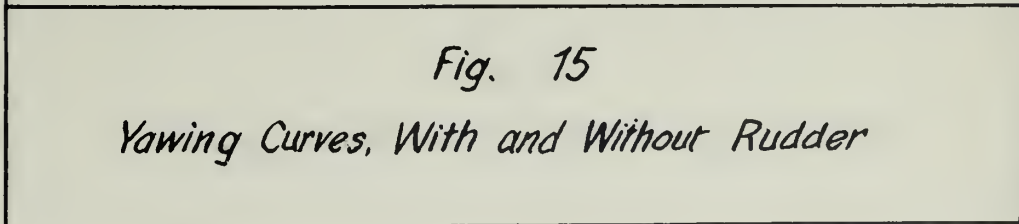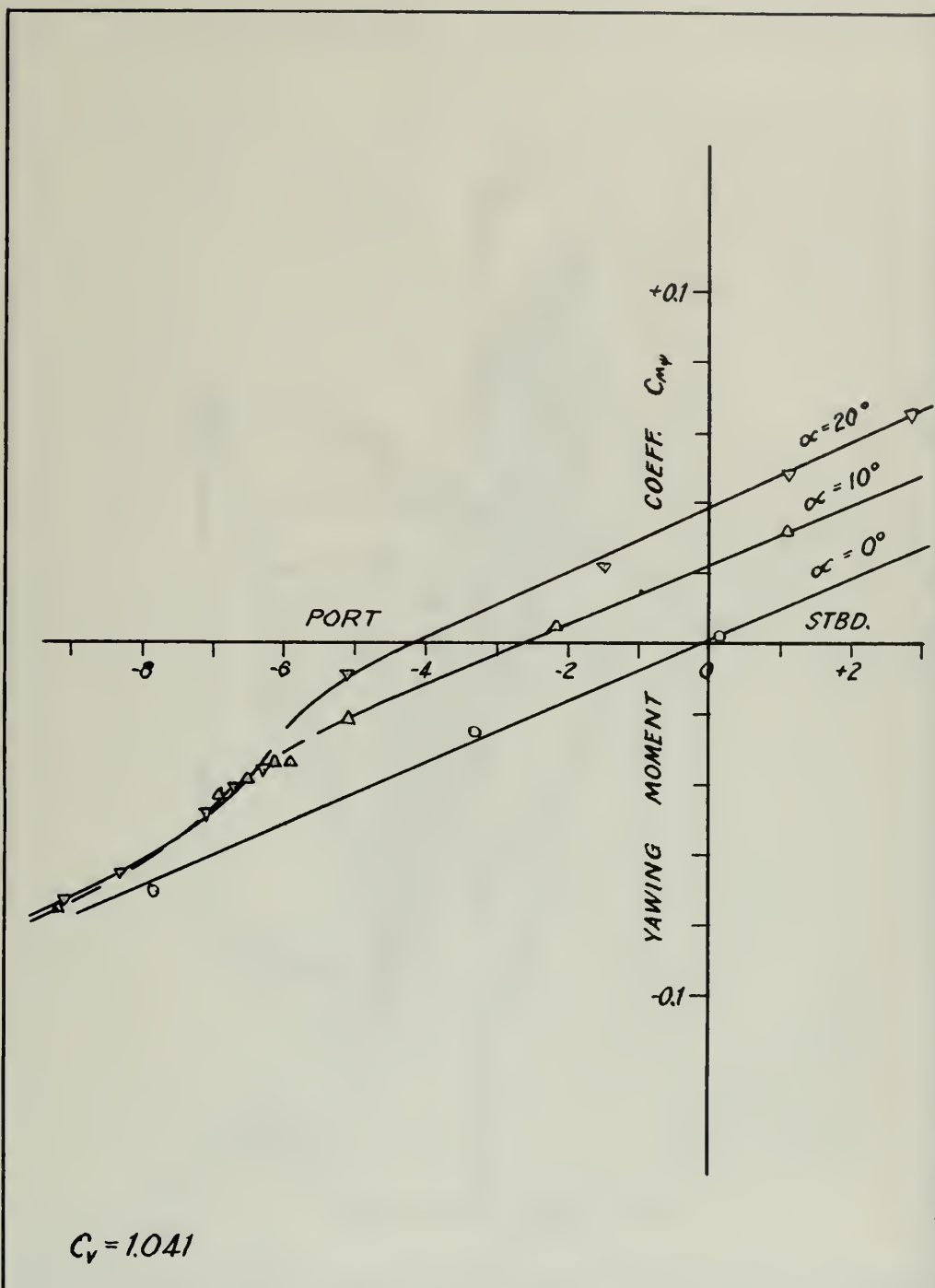
Fig. 16

Yawing Curves at Rudder Angles, A=1.0

$$\alpha = \psi + \alpha_H + \epsilon$$
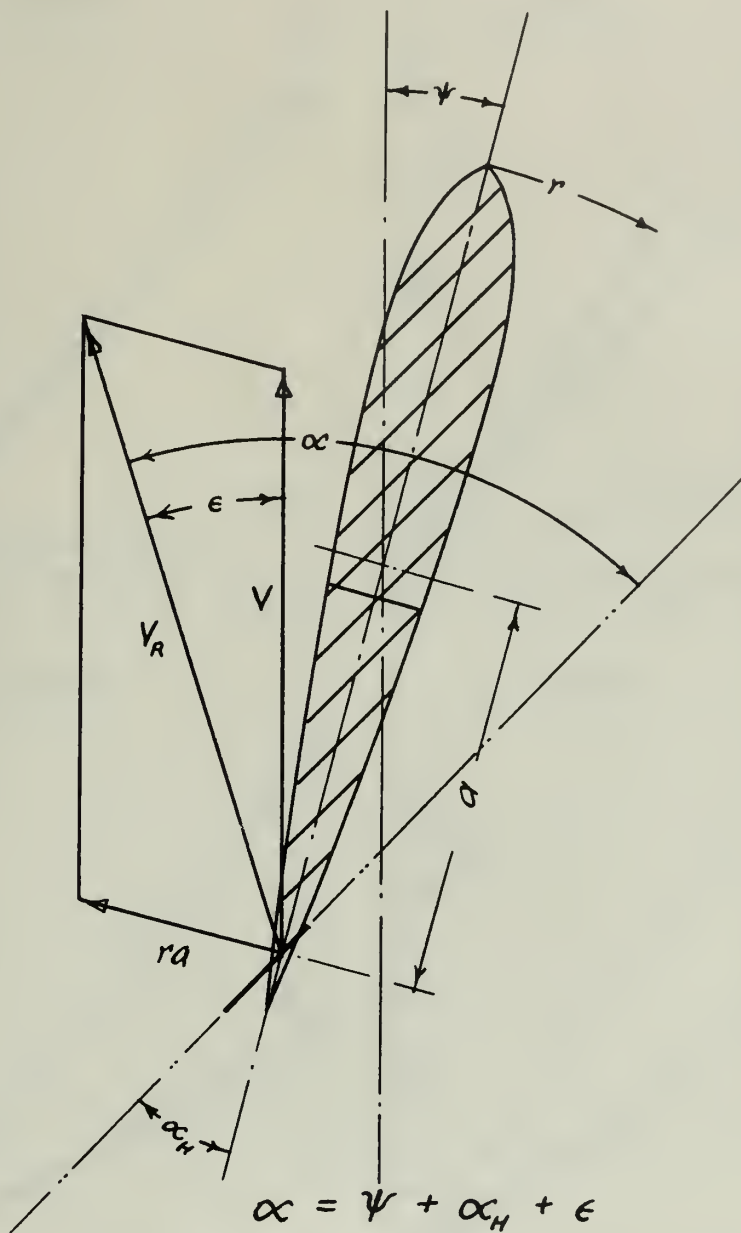
Fig. 17

Effect of Yaw on Rudder Angle of Attack
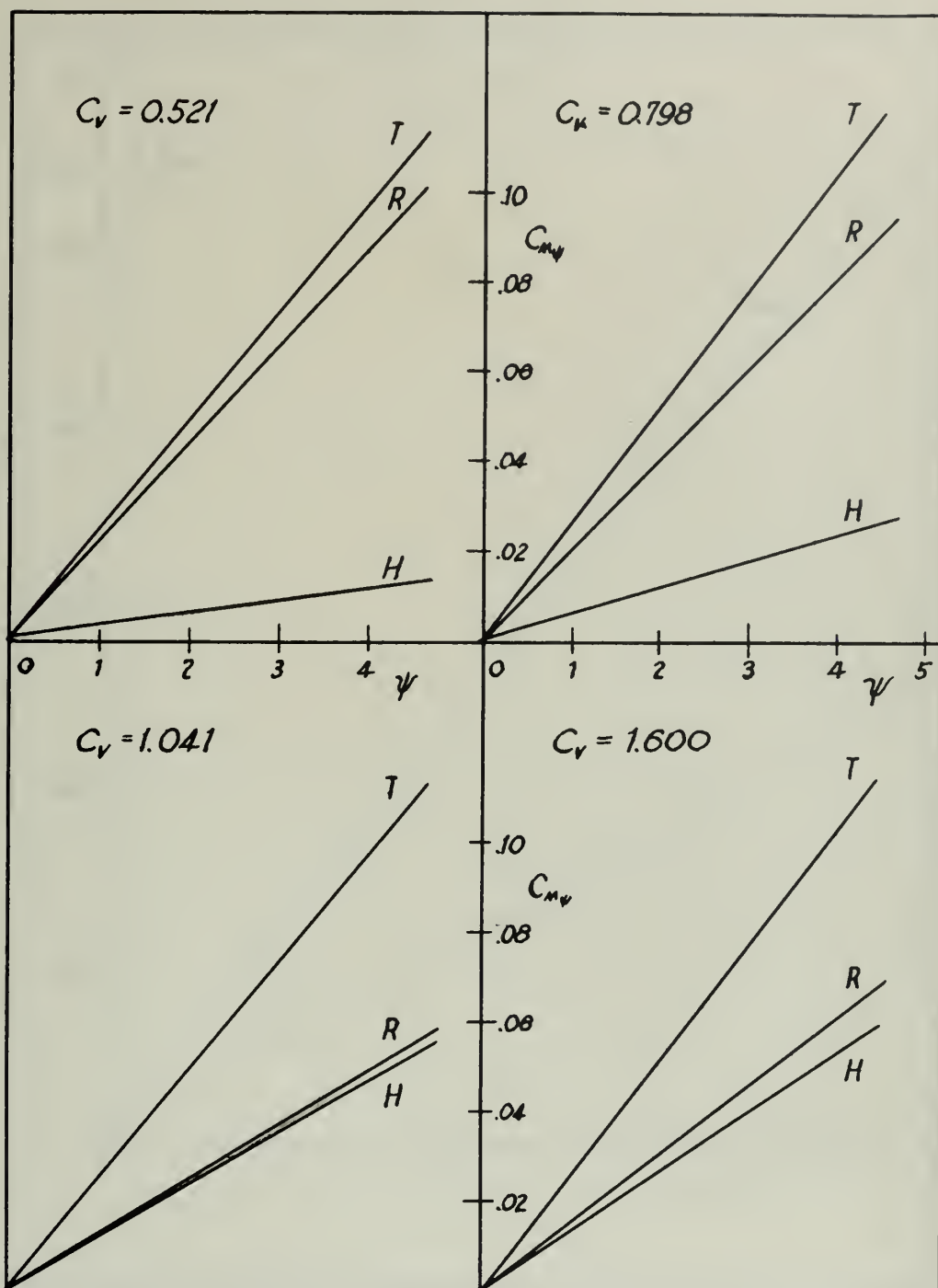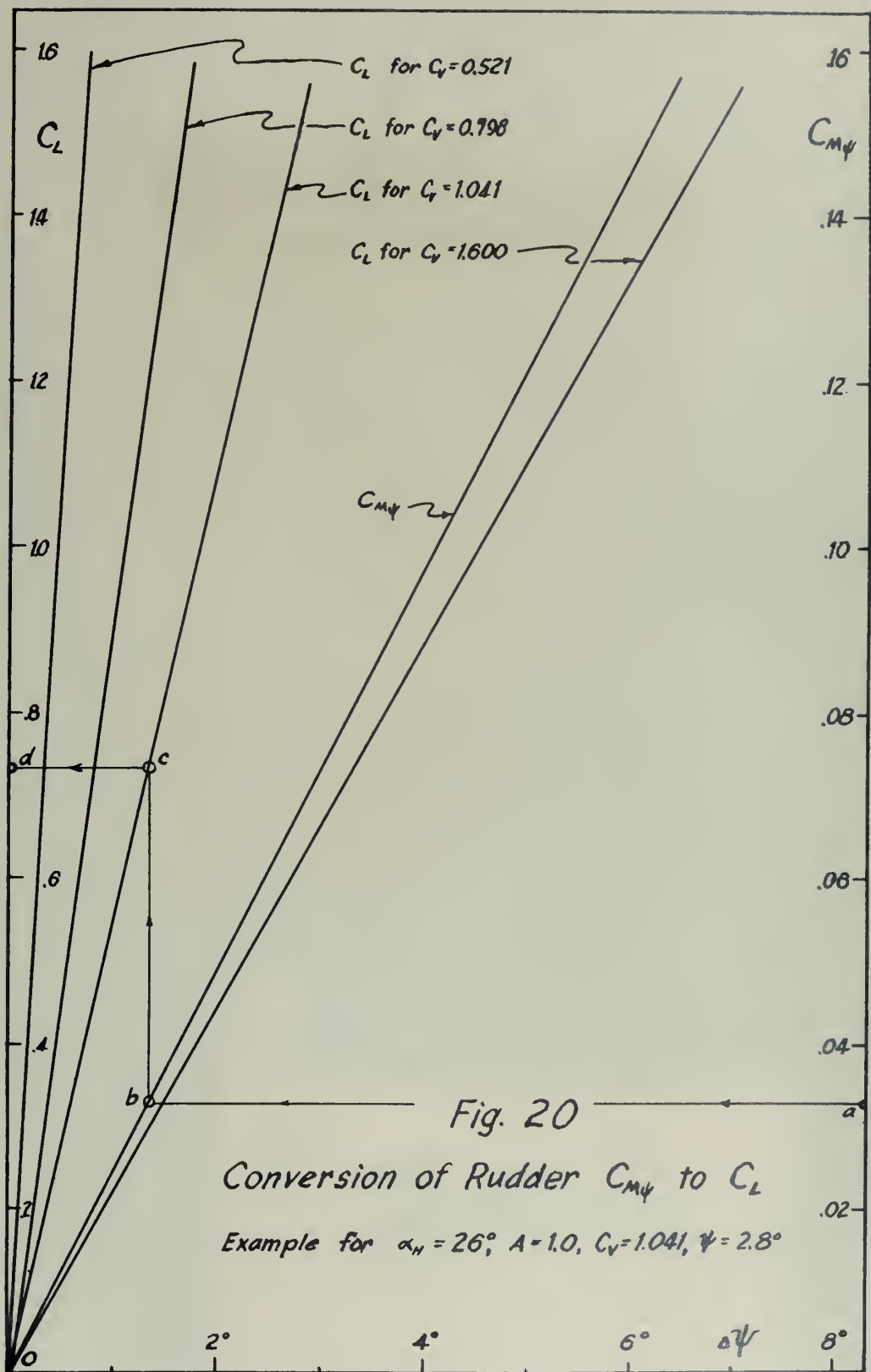
Fig. 18

Graphical Solution of Rudder Alone Curve
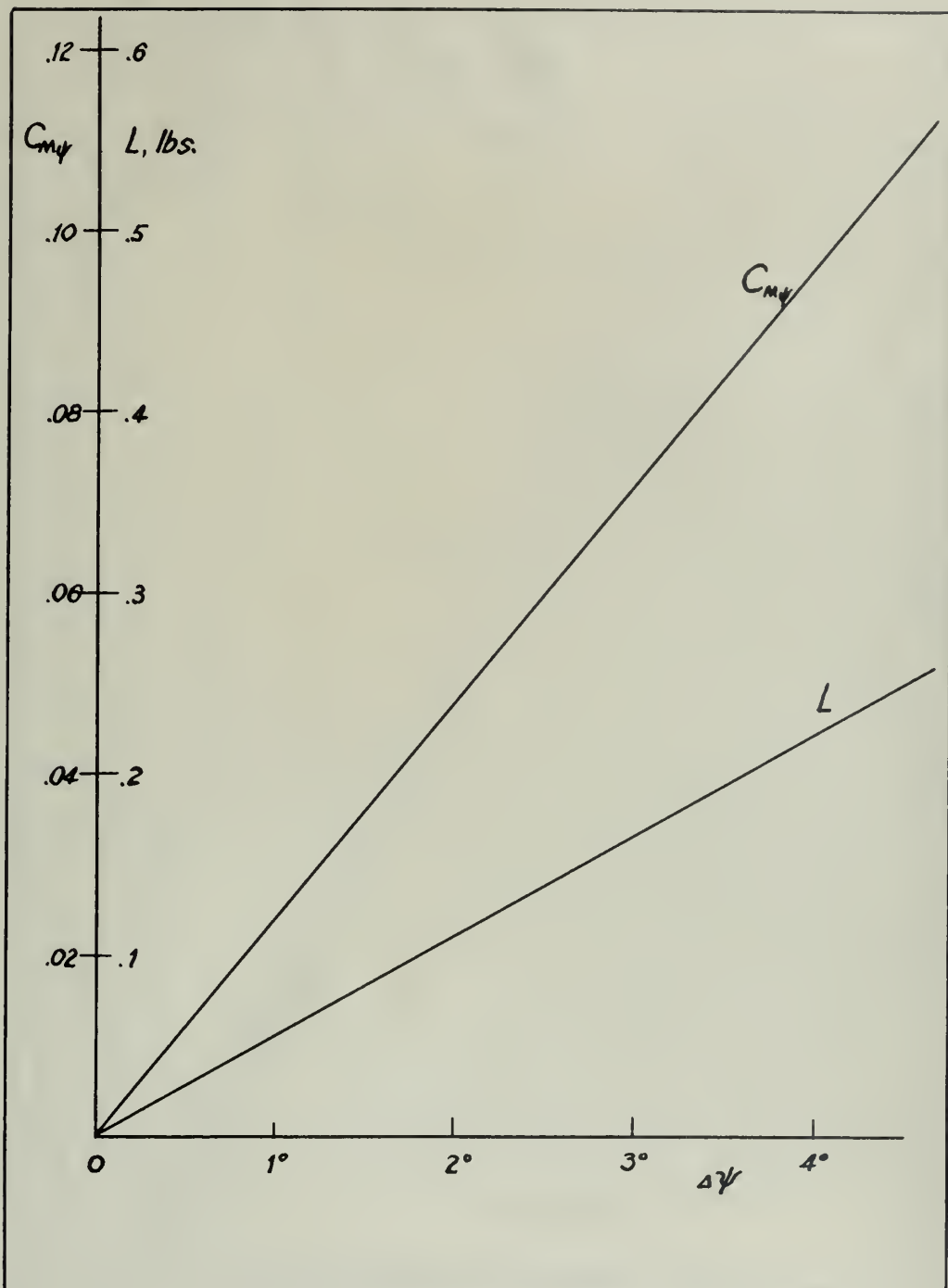
Fig. 19

Spring Calibration Curves

Fig. 20

Conversion of Rudder $C_{M\psi}$ to C_L

Example for $\alpha_H = 26°$, $A = 1.0$, $C_V = 1.041$, $\psi = 2.8°$

C_L for $C_V = 0.521$

C_L for $C_V = 0.798$

C_L for $C_V = 1.041$

C_L for $C_V = 1.600$

$C_{M\psi}$

C_L

$C_{M\psi}$

$\Delta \psi$